Band magnetism in the Hubbard model

W. Nolting and W. Borgiel*
Max-Planck-Institut für Plasmaphysik, Boltzmannstrasse 2, D-8046 Garching, Federal Republic of Germany
(Received 13 September 1988)

A self-consistent moment method is applied to the Hubbard model in order to find out under what circumstances spontaneous band magnetism may occur. The theory is formulated for a two-sublattice structure to treat simultaneously para-, ferro-, and antiferromagnetic systems. The starting point is a two-pole ansatz for the one-electron spectral density, the free parameters of which are fitted by equating exactly calculated spectral moments. All correlation functions appearing in the moments can be expressed by the spectral density, guaranteeing therewith a closed system of equations, which can be solved self-consistently for the average particle numbers $\langle n_{i\uparrow}\rangle$ and $\langle n_{i\downarrow}\rangle$. A $T=0$ phase diagram is presented in terms of band occupation n ($0\leq n\leq 2$) and Coulomb interaction U. Ferromagnetic solutions appear only if n exceeds a critical occupation n_c^{FM} and U a minimum value $U_{\min}$. For antiferromagnetic solutions a critical U does not exist, but a critical band occupation n_c^{AFM} does. Antiferromagnetism is stable in a restricted region of n around $n=1$, which is broadest for intermediate couplings ($U/W\cong 1$, W being the Bloch bandwidth) and shrinks to the $n=1$ axis for strong couplings ($U/W\rightarrow\infty$). For smaller n, but $n>n_c^{\mathrm{FM}}$ and sufficiently high U ($U>W$), ferromagnetism is stable, while for low band occupations the system is paramagnetic irrespective of U. The critical temperatures T_C and T_N are strongly U and n dependent. For fixed n, T_C increases with U, but saturates for $U\rightarrow\infty$ at finite values (500–800 K), while T_N has a maximum at an intermediate U value ($U\cong W$). First-order as well as second-order transitions are observed. Ferromagnetic order arises mainly because of a shift of $\uparrow$ and $\downarrow$ quasiparticle subbands. In antiferromagnets, corresponding $\uparrow$ and $\downarrow$ subbands occupy exactly the same energy regions, but with different state densities. The magnetic behavior of the Hubbard model can be understood as a direct consequence of the sensitive (T,n,U) dependence of the quasiparticle density of states, which is therefore discussed in detail.

I. INTRODUCTION

The so-called Hubbard model,[1–3] which describes a single s band with local electron-electron repulsion is commonly used for the study of strongly correlated electrons in a narrow energy band. This model is thought to be able to reproduce cooperative phenomena like spontaneous band magnetism[4] or insulator-metal transitions[5] ("Mott-Hubbard transitions"). In the very recent past the Hubbard model has furthermore become a weighty candidate for the theoretical explanation of high-T_c superconductivity.[6]

Despite the rather simple structrue of the model Hamiltonian (Sec. II A) the general solution of the respective many-body problem is not yet available. Unavoidable approximations have led to partially contradicting statements. It is therefore fair to say that the true inherent model properties have not yet been worked out unambiguously up to now. In this paper we contribute to a clarification, where our special interest aims at the question of whether or not spontaneous ferro- or antiferroband magnetisim may appear in the Hubbard model. In a previous paper[7] one of us has shown by use of a self-consistent moment method for the strongly correlated Hubbard model that under certain conditions, concerning band occupation and lattice structure, ferromagnetism is stable against paramagnetism. We are going to present an extension of this theory to arbitrary correlation strengths including antiferromagnetic structures. Great effort has been devoted by many authors to the ground-state properties of the Hubbard model; relatively few studies, however, refer to finite-temperature properties, in particular to the transition temperatures (T_C,T_N) of the magnetically ordered system. Our study covers both aspects.

Of great importance for testing unavoidable approximations are exactly solvable limiting cases. Unfortunately, only few are available. The one-dimensional Hubbard model has been solved by Lieb and Wu[8] for $T=0$ and arbitrary band occupation n ($0\leq n\leq 2$), and by Beni *et al*[9] for finite temperatures in the $U\rightarrow\infty$ limit. But these results provide only very restricted information about the three-dimensional system, notably because it can exactly be shown that collective magnetic order is impossible for $T>0$ in the one- and two-dimensional Hubbard model.[10,11] For the three-dimensional case Nagaoka[12] has presented rigorous ($T=0, U\rightarrow\infty$) results for the special band fillings $n=n_{\mp}=1/N(N\mp 1)$ (N is number of lattice sites). sc and bcc lattices have ferromagnetic ground states for n_+ as well as n_-, the fcc lattice only for n_+. These results, however, have been criticized as meaningless in the thermodynamic limit,[13] although being in remarkable agreement with some reliable approximate theories.[14–16] No doubt exists, however, about low band occupations ($n\ll 1$), for which no collective magnetic order is expected.[17] If at all, then magnetism becomes like-

ly in a certain n region around the half-filled band ($n=1$). For the narrow-band limit, where the hopping integral may be considered as a small perturbation compared to the intraatomic Coulomb matrix element, Anderson[18] has used second-order perturbation theory to transform the Hubbard model for exactly half-filled bands into an effective Heisenberg model. In this special case ($n=1$) antiferromagnetism is predicted.

An immense variety of approximate theories has been proposed in the past, based, e.g., on mean-field approximations,[19,20] Green's-function techniques,[1,14,16,21] functional integral methods,[22–29] variational approaches,[30,31] and fourth-order perturbation expansions.[32,33] As already mentioned, not all results are sound, but practically all of them predict that collective magnetism is possible in the three-dimensional Hubbard model. Interesting information can be drawn from the investigation of finite systems, performed for chains[34,35] typically up to 12 sites, for an 8×8 square lattice,[36] and for three-dimensional clusters,[37,38] e.g., $4\times4\times4$ or $6\times6\times6$. It is, however, surely fair to question, whether these systems are large enough to allow conclusions about the model properties in the thermodynamic limit.

We investigate in this paper the possibility of spontaneous ferro- or antiferromagnetism within the framework of the Hubbard model. For this purpose we apply a self-consistent moment method,[7] which we call the "spectral-density approach" (SDA). Previous applications[39–41] have evidenced the SDA to be a powerful tool for solving menay-body problems. The main advantages are the very simple concept of the method[41] and its nonperturbative character, which makes it useful in particular for systems with phase transitions. Restricting our considerations to lattices which consists of two interpenetrating sublattices A and B, we derive with the SDA a closed set of equations, which is self-consistently solved for the average particle numbers $\langle n_{\alpha\uparrow}\rangle$ and $\langle n_{\alpha\downarrow}\rangle$. The index α stands for A and B, respectively. Spontaneous band magnetism is indicated by $\langle n_{\alpha\uparrow}\rangle\neq\langle n_{\alpha\downarrow}\rangle$ with $\langle n_{A\sigma}\rangle=\langle n_{B\sigma}\rangle$ for ferromagnet and $\langle n_{A\sigma}\rangle=\langle n_{B-\sigma}\rangle$ for the antiferromagnet.

Band magnetism is very often discussed in terms of the so-called Stoner model, which is just the mean-field approximation of the Hubbard model. We believe, however, that this approach is quite misleading, at least what concerns finite-temperature properties of strongly correlated electron systems. This can be demonstrated by the quasiparticle density of states $\rho_\sigma(E)$ (QDOS). For fixed model parameters (lattice structure, Coulomb interaction U, Bloch bandwidth W) this fundamental quantity depends very sensitively on temperature T and band occupation n ($0\leq n\leq2$). As an example, the Stoner model predicts for a ferromagnetic lattice a rigid shifting of the $\uparrow$ and $\downarrow$ spectra of Um. Here m denotes the average magnetic moment per site. The exchange splitting is, therefore, temperature dependent, starting at value Un for $T=0$, which typically means several eV, and disappearing for $T\geq T_C$. The huge $T=0$ gap, which has to be closed for $T\rightarrow T_C$ causes an extremely high Curie temperature T_C. This well-known shortcoming of the Stoner theory is completely due to the wrong QDOS. In the SDA we shall derive that the excitation spectrum is split for all temperatures into a low- and high-energy part, the distance of which is only slightly temperature dependence. For $T<T_C$ there appears an additional, nonrigid spin splitting of *both* parts, which results in a temperature-dependent spontaneous magnetization. This QDOS structure leads to realistic orders of magnitude for T_C, where T_C is a function of n and U/W. Similar disprepancies between the results of the Stoner theory and SDA exist for antiferromagnetic systems.

We have organized our paper as follows. In Sec. II the model Hamiltonian is formulated for the two-sublattice structure, followed by an inspection of the "free" ($U=0$) system, which will be used as a starting point for our self-consistent moment method. To get a first insight into the physics of the not exactly solvable Hubbard model we subsequently present results of the Stoner theory in the form of a $T=0$ phase diagram, and of temperature-dependent QDOS for ferro- and antiferromagnetic electron systems. In Sec. III we develop our moment method (SDA), showing, e.g., how it can be made self-consistent by expressing higher correlation functions by the one-electron spectral density. The results are presented and discussed in Sec. IV.

II. HUBBARD MODEL

A. Model Hamiltonian

Usually band magnetism is theoretically investigated within the framework of the Hubbard model,[1–3,13] which is believed to describe in a rather realistic manner the properties of correlated electrons in a narrow energy band. Since our study aims simultaneously at ferro- and antiferromagnetism in the Hubbard model, we decompose the total lattice into m chemically equivalent sublattices ($\alpha=1,2,\ldots,m$), and describe it as a "magnetic" Bravais lattice ($\mathbf{R}_i$) with an m-atom basis ($\mathbf{r}_\alpha$). The position vectors of the constituents of the original ("chemical") lattice are then given by

$$\mathbf{R}_{i\alpha}=\mathbf{R}_i+\mathbf{r}_\alpha\ , \tag{2.1}$$

where i numbers the N sites of the magnetic Bravais lattice, and α the m basis atoms, each of which belongs to one of the m sublattices. Fourier transformation between local space and $\mathbf{k}$ space will be done in the Bravais lattice only. Operators, e.g., are transformed as follows:

$$O_{i\alpha}=N^{-1/2}\sum_{\mathbf{k}}e^{i\mathbf{k}\cdot\mathbf{R}_i}O_{\mathbf{k}\alpha}\ , \tag{2.2}$$

$$O_{\mathbf{k}\alpha}=N^{-1/2}\sum_{\mathbf{k}}e^{-i\mathbf{k}\cdot\mathbf{R}_i}O_{i\alpha}\ . \tag{2.3}$$

$\mathbf{k}$ is a wave vector of the first Brillouin zone of the Bravais lattice. This possesses translational symmetry, so that the thermodynamic average of the operator $O_{i\alpha}$ does not depend on site $\mathbf{R}_i$

$$\langle O_{i\alpha}\rangle\equiv\langle O_\alpha\rangle\forall i\ . \tag{2.4}$$

We cannot exclude, however, a sublattice (α) dependence. Taking into account such a sublattice structure the Hub-

bard Hamiltonian reads as

$$H=\sum_{\substack{i,j,\sigma\\ \alpha,\beta}} T_{ij}^{\alpha\beta} c_{i\alpha\sigma}^{\dagger} c_{j\beta\sigma} + \tfrac{1}{2} U \sum_{\substack{i,\sigma\\ \alpha}} n_{i\alpha\sigma} n_{i\alpha-\sigma} \; . \tag{2.5}$$

$c_{i\alpha\sigma}^{\dagger}(c_{i\alpha\sigma})$ is the creation (annihilation) operator of an electron with spin σ in a Wannier state at site $\mathbf{R}_{i\alpha}$. $n_{i\sigma}=c_{i\alpha\sigma}^{\dagger}c_{i\alpha\sigma}$ is the number operator, and U the intra-atomic Coulomb matrix element. The hopping integrals $T_{ij}^{\alpha\beta}$,

$$T_{ij}^{\alpha\beta}=\frac{1}{N}\sum_{\mathbf{k}} \varepsilon_{\alpha\beta}(\mathbf{k}) e^{i\mathbf{k}\cdot(\mathbf{R}_i-\mathbf{R}_j)} \; , \tag{2.6}$$

as well as the Bloch energies $\varepsilon_{\alpha\beta}(\mathbf{k})$ contain the kinetic energy of the band electrons and the influence of the periodic lattice potential. In what follows we consider exclusively lattices with $AB\,AB$ structure, i.e., two sublattices A and B penetrating each other in such a way that all nearest neighbors of an A atom are from sublattice B and vice versa. The electron hopping shall take place between nearest (Δ_1) and next-nearest (Δ_2) neighbors in the chemical lattice

$$T_{ij}^{\alpha\beta}=\begin{cases} T_0 & \text{if } \mathbf{R}_{i\alpha}=\mathbf{R}_{j\beta} \\ t_1 & \text{if } \mathbf{R}_{i\alpha}-\mathbf{R}_{j\beta}=\Delta_1 \\ t_2 & \text{if } \mathbf{R}_{i\alpha}-\mathbf{R}_{j\beta}=\Delta_2 \\ 0 & \text{otherwise} \; . \end{cases} \tag{2.7}$$

Hopping between nearest neighbors of a chemical lattice with ABAB structure always means intersublattice hopping,

$$\varepsilon_{AB}(\mathbf{k})=t_1 e^{i\mathbf{k}\cdot(\mathbf{r}_A-\mathbf{r}_B)}\sum_{\Delta_1} e^{-i\mathbf{k}\cdot\Delta_1}\equiv t(\mathbf{k}) \; , \tag{2.8}$$

$$\varepsilon_{BA}(\mathbf{k})=t^{*}(\mathbf{k}) \; . \tag{2.9}$$

Formally, $|t(\mathbf{k})|$ is the tight-binding approximation for the Bloch energies of the chemical lattice, but with $\mathbf{k}$ from the Brillouin zone of the magnetic lattice. Hopping between next-nearest neighbors means hopping within a given sublattice

$$\varepsilon_{AA}(\mathbf{k})=\varepsilon_{BB}(\mathbf{k})=t_2\sum_{\Delta_2} e^{-i\mathbf{k}\cdot\Delta_2}\equiv\varepsilon(\mathbf{k}) \; , \tag{2.10}$$

$\varepsilon(\mathbf{k})$ turns out to be the tight-binding approximation for the Bloch energies of the magnetic Bravais lattice.

The main goal of our study is to find out whether or not ferromagnetism and antiferromagnetism, respectively, may be possible within the framework of the Hubbard model. We shall investigate, for which Coulomb interactions U, band occupations n ($0\le n\le 2$), and lattice structures the sublattice magnetization

$$m_A=\langle n_{A\uparrow}\rangle-\langle n_{A\downarrow}\rangle\equiv m \tag{2.11}$$

becomes unequal zero. We assume that each sublattice orders ferromagnetically, if at all, but so that

$$m_A=m_B \text{ ferromagnet} \; , \tag{2.12}$$

$$m_A=-m_B \text{ antiferromagnet} \tag{2.13}$$

holds.

The decisive quantity for our procedure will be the one-electron spectral density.

$$S_{\mathbf{k}\sigma}^{\alpha\beta}(E)=\frac{1}{N}\sum_{i,j} S_{ij\sigma}^{\alpha\beta}(E) e^{-i\mathbf{k}\cdot(\mathbf{R}_i-\mathbf{R}_j)} \; , \tag{2.14}$$

$$S_{ij\sigma}^{\alpha\beta}(E)=\int_{-\infty}^{+\infty} d(t-t') e^{i/\hbar E(t-t')} \times\frac{1}{2\pi}\langle [c_{i\alpha\sigma}(t),c_{j\beta\sigma}^{\dagger}(t')]_{+}\rangle \; . \tag{2.15}$$

By use of the spectral theorem[42] the average occupation numbers needed in (2.11) are directly determined by the spectral density

$$\langle n_{\alpha\sigma}\rangle=\int_{-\infty}^{+\infty} dE\, f_{-}(E) S_{ii\sigma}^{\alpha\alpha}(E) \; , \tag{2.16}$$

$$f_{-}(E)=(e^{\beta(E-\mu)}+1)^{-1} \; . \tag{2.17}$$

A further important quantity is the quasiparticle density of states (QDOS)

$$\rho_{\sigma}(E)=\frac{1}{2N\hbar}\sum_{i,\alpha} S_{ii\sigma}^{\alpha\alpha}(E)=\frac{1}{2}\sum_{\alpha}\frac{1}{N\hbar}\sum_{\mathbf{k}} S_{\mathbf{k}\sigma}^{\alpha\alpha}(E) \; . \tag{2.18}$$

We define

$$\rho_{\alpha\sigma}(E)=\frac{1}{N\hbar}\sum_{i} S_{ii\sigma}^{\alpha\alpha}(E)=\frac{1}{N\hbar}\sum_{\mathbf{k}} S_{\mathbf{k}\sigma}^{\alpha\alpha}(E) \tag{2.19}$$

as the α sublattice QDOS. Because of general sysmmetry we have to assume

$$\begin{aligned} &\rho_{A\sigma}(E)=\rho_{B\sigma}(E) \quad \text{ferromagnet} \; , \\ &\rho_{A\sigma}(E)=\rho_{B-\sigma}(E) \quad \text{antiferromagnet} \; . \end{aligned} \tag{2.20}$$

In the case of the ferromagnet total QDOS $\rho_{\sigma}(E)$ and sublattice QDOS $\rho_{\alpha\sigma}(E)$ are, of course, identical.

B. The "free" system

We first inspect the free ($U=0$) system, because it will be the starting point for our self-consistent moment method. It is defined by

$$H_0=\sum_{\substack{i,j,\sigma\\ \alpha,\beta}} T_{ij}^{\alpha\beta} c_{i\alpha\sigma}^{\dagger} c_{j\beta\sigma}=\sum_{\substack{\mathbf{k},\sigma\\ \alpha,\beta}} \varepsilon_{\alpha\beta}(\mathbf{k}) c_{\mathbf{k}\alpha\sigma}^{\dagger} c_{\mathbf{k}\beta\sigma} \; . \tag{2.21}$$

In order to diagonalize H_0,

$$H_0=\sum_{\mathbf{k},\sigma,p} \eta_p(\mathbf{k}) d_{\mathbf{k}\sigma p}^{\dagger} d_{\mathbf{k}\sigma p} \quad (p=\mp) \; . \tag{2.22}$$

We introduce new one-particle construction operators $d_{\mathbf{k}\sigma p}, d_{\mathbf{k}\sigma p}^{\dagger}$,

$$d_{\mathbf{k}\sigma p}=\gamma_{Ap} c_{\mathbf{k}A\sigma}+\gamma_{Bp} c_{\mathbf{k}B\sigma} \; , \tag{2.23}$$

$$d_{\mathbf{k}\sigma p}^{\dagger}=\gamma_{Ap}^{*} c_{\mathbf{k}A\sigma}^{\dagger}+\gamma_{Bp}^{*} c_{\mathbf{k}B\sigma}^{\dagger} \; . \tag{2.24}$$

They shall obey the usual Fermi anticommutator rules,

$$[d_{\mathbf{k}\sigma p}, d_{\mathbf{k}'\sigma' p'}^{\dagger}]_{+}=\delta_{\mathbf{k}\mathbf{k}'}\delta_{\sigma\sigma'}\delta_{pp'} \; , \tag{2.25}$$

$$[d_{k\sigma p}, d_{\mathbf{k}'\sigma' p'}]_{+}=0 \tag{2.26}$$

implying therewith for the coefficients γ_{Ap}, γ_{Bp},

$$|\gamma_{Ap}|^2+|\gamma_{Bp}|^2=1,\quad \gamma_{A+}\gamma_{A-}^*+\gamma_{B+}\gamma_{B-}^*=0\ . \tag{2.27}$$

The commutator of $d_{\mathbf{k}\sigma p}$ with H_0 can be calculated in a twofold manner, namely by use of (2.22),

$$[d_{\mathbf{k}\sigma p},H_0]_-=\eta_p(\mathbf{k})(\gamma_{Ap}c_{\mathbf{k}A\sigma}+\gamma_{Bp}c_{\mathbf{k}B\sigma}) \tag{2.28}$$

as well as with (2.21)

$$[d_{\mathbf{k}\sigma p},H_0]_-=\gamma_{Ap}[\varepsilon(\mathbf{k})c_{\mathbf{k}A\sigma}+t(\mathbf{k})c_{\mathbf{k}B\sigma}] +\gamma_{Bp}[\varepsilon(\mathbf{k})c_{\mathbf{k}B\sigma}+t^*(\mathbf{k})c_{\mathbf{k}A\sigma}]\ . \tag{2.29}$$

The last two equations provoke the following homogeneous system of equations:

$$\begin{aligned}&\gamma_{Ap}[\varepsilon(\mathbf{k})-\eta_p(\mathbf{k})]+\gamma_{Bp}t^*(\mathbf{k})=0\ ,\\ &\gamma_{Ap}t(\mathbf{k})+\gamma_{Bp}[\varepsilon(\mathbf{k})-\eta_p(\mathbf{k})]=0\ ,\end{aligned} \tag{2.30}$$

the secular equation of which is solved by,

$$\eta_p(\mathbf{k})=\varepsilon(\mathbf{k})+p|t(\mathbf{k})|\quad (p=\mp)\ . \tag{2.31}$$

Equations (2.27), (2.30), and (2.31) determine the coefficients $\gamma_{A,Bp}$, and therewith the transformation (2.23) and (2.24):

$$d_{\mathbf{k}\sigma p}=(\tfrac{1}{2})^{1/2}\{c_{\mathbf{k}A\sigma}+p[t(\mathbf{k})/|t(\mathbf{k})|]c_{\mathbf{k}B\sigma}\}\ , \tag{2.32}$$

$$d^\dagger_{\mathbf{k}\sigma p}=(\tfrac{1}{2})^{1/2}\{c^\dagger_{\mathbf{k}A\sigma}+p[t^*(\mathbf{k})/|t(\mathbf{k})|]c^\dagger_{\mathbf{k}B\sigma}\}\ . \tag{2.33}$$

The reversion reads

$$c_{\mathbf{k}A\sigma}=(\tfrac{1}{2})^{1/2}(d_{\mathbf{k}\sigma+}+d_{\mathbf{k}\sigma-})\ , \tag{2.34}$$

$$c_{\mathbf{k}B\sigma}=(\tfrac{1}{2})^{1/2}(d_{\mathbf{k}\sigma+}-d_{\mathbf{k}\sigma-})|t(\mathbf{k})|/t(\mathbf{k})\ . \tag{2.35}$$

By use of these d operators we can define two new one-particle spectral densities

$$A_{\mathbf{k}\sigma p}(E)=\int_{-\infty}^{+\infty}d(t-t')e^{i/\hbar E(t-t')}\frac{1}{2\pi} \times\langle[d_{\mathbf{k}\sigma p}(t),d^\dagger_{\mathbf{k}\sigma p}(t')]_+\rangle\ , \tag{2.36}$$

$$D^{p,-p}_{\mathbf{k}\sigma}(E)=\int_{-\infty}^{+\infty}d(t-t')e^{i/\hbar E(t-t')}\frac{1}{2\pi} \times\langle[d_{\mathbf{k}\sigma p}(t),d^\dagger_{\mathbf{k}\sigma -p}(t')]_+\rangle\ . \tag{2.37}$$

The connection with the "original" spectral densities $S^{\alpha\beta}_{\mathbf{k}\sigma}(E)$, defined in (2.14), follows directly with (2.34) and (2.35),

$$S^{AA}_{\mathbf{k}\sigma}(E)=\tfrac{1}{2}\sum_p[A_{\mathbf{k}\sigma p}(E)+D^{(p,-p)}_{\mathbf{k}\sigma}(E)]\ , \tag{2.38}$$

$$S^{BB}_{\mathbf{k}\sigma}(E)=\tfrac{1}{2}\sum_p[A_{\mathbf{k}\sigma p}(E)-D^{(p,-p)}_{\mathbf{k}\sigma}(E)]\ , \tag{2.39}$$

$$S^{AB}_{\mathbf{k}\sigma}(E)=\tfrac{1}{2}[|t(\mathbf{k})|/t^*(\mathbf{k})] \times\sum_p p[A_{\mathbf{k}\sigma p}(E)-D^{(p,-p)}_{\mathbf{k}\sigma}(E)]\ , \tag{2.40}$$

$$S^{BA}_{\mathbf{k}\sigma}(E)=\tfrac{1}{2}[|t(\mathbf{k})|/t(\mathbf{k})] \times\sum_p p[A_{\mathbf{k}\sigma p}(E)+D^{(p,-p)}_{\mathbf{k}\sigma}(E)]\ . \tag{2.41}$$

We shall use these relations several times at a later stage of this paper.

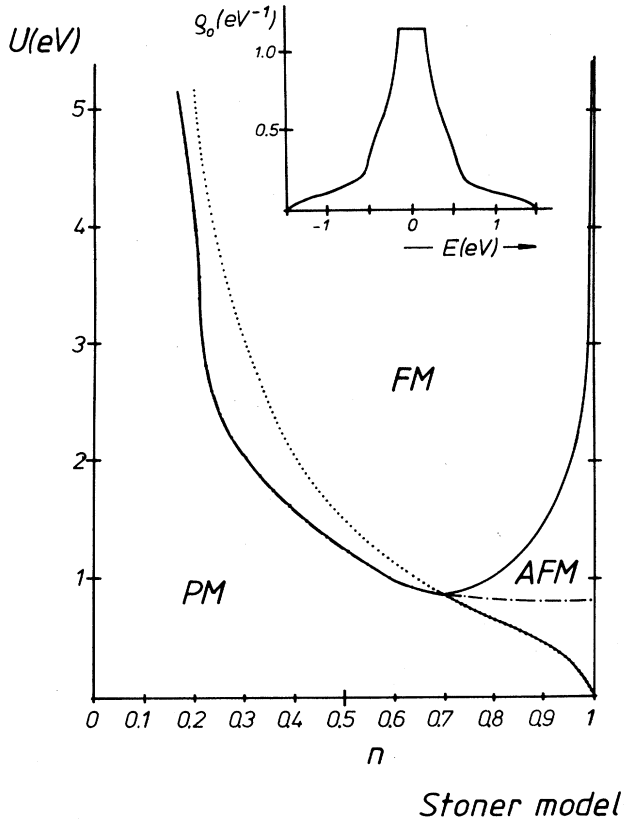

FIG. 1. $T=0$ phase diagram of the Stoner model in terms of Coulomb interaction U and band occupation n. Solid lines are the phase boundaries between paramagnetism (PM), ferromagnetism (FM), and antiferromagnetism (AFM). Ferromagnetic (antiferromagnetic) solutions exist above the dashed-dotted (dotted) line. The phase diagram is symmetric to the $n=1$ axis. The $1\le n\le 2$ region is, therefore, attainable by reflection on the $n=1$ axis. The inset shows the Bloch density of states ρ_0 of the free ($U=0$) system as function of energy. The bandwidth W is 3 eV.

For the free system ($U=0$) the functions A and D are especially simple. Because of

$$d_{\mathbf{k}\sigma p}(t)=d_{\mathbf{k}\sigma p}e^{-i/\hbar\eta_p(\mathbf{k})t}\ , \tag{2.42}$$

we find with (2.25)

$$\begin{aligned}&A^{(0)}_{\mathbf{k}\sigma p}(E)=\hbar\delta(E-\eta_p(\mathbf{k}))\ ,\\ &{}^{(0)}D^{(p,-p)}_{\mathbf{k}\sigma}(E)\equiv 0\ .\end{aligned} \tag{2.43}$$

The upper index 0 shall indicate the $U=0$ case. For the interacting system ($U\neq 0$) (2.42) is no longer valid. A and D then become very much more complicated.

With (2.42) in (2.38) and (2.39), respectively, we can formulate the so-called Bloch density of states (BDOS) $\rho_0(E)$,

$$\rho^{(0)}_{A\sigma}(E)=\rho^{(0)}_{B\sigma}(E) \equiv\rho_0(E)=\frac{1}{2N}\sum_{\mathbf{k}}\sum_p\delta(E-\eta_p(\mathbf{k}))\ . \tag{2.44}$$

The **k** summation runs over the first Brillouin zone of the magnetic Bravais lattice.

The actual evaluation of our theory, which we are going to present, will be performed with

$$\varepsilon(\mathbf{k})=\tfrac{1}{6}[\cos(k_x a)+\cos(k_y a)+\cos(k_z a)] \tag{2.45}$$

(a is the Bravais-lattice constant), and

$$t(\mathbf{k})=2\varepsilon(\mathbf{k}) . \tag{2.46}$$

The resulting BDOS is plotted as the inset in Fig. 1. The total bandwidth W is 3 eV.

C. Stoner model

In order to get a first insight into the physics of the not exactly solvable Hubbard model, let us have a short look at the simplest approximation, which uses a mean-field diagonalization of the Coulomb interaction term (Stoner model),

$$H_S=\sum_{i,j,\sigma} T_{ij\sigma}^{\alpha\beta} c_{i\alpha\sigma}^{\dagger} c_{j\beta\sigma} = \sum_{\mathbf{k}\sigma} \varepsilon_{\alpha\beta\sigma}(\mathbf{k}) c_{\mathbf{k}\alpha\sigma}^{\dagger} c_{\mathbf{k}\beta\sigma} , \tag{2.47}$$

$$T_{ij\sigma}^{\alpha\beta}=T_{ij}^{\alpha\beta}+U\langle n_{\alpha-\sigma}\rangle\delta_{ij}\delta_{\alpha\beta} . \tag{2.48}$$

This model Hamiltonian has the same structure as H_0 in (2.21). We can, therefore, diagonalize H_S strictly along the line, sketched for H_0 in Sec. II B. After simple manipulations one finds the following sublattice QDOS:

$$\rho_{A\sigma}^{(S)}(E)=\frac{1}{N}\sum_{\mathbf{k}}\sum_{p=\mp}\gamma_{\sigma p}(\mathbf{k})\delta(E-E_{\sigma p}(\mathbf{k})) . \tag{2.49}$$

$\rho_{B\sigma}^{(S)}(E)$ follows from $\rho_{A\sigma}^{(S)}(E)$ according to (2.20). The quasiparticle energies $E_{\sigma p}(\mathbf{k})$

$$E_{\sigma p}(\mathbf{k})=\varepsilon(\mathbf{k})+\tfrac{1}{2}U(\langle n_{A-\sigma}\rangle+\langle n_{B-\sigma}\rangle) +p[\tfrac{1}{4}U^2(\langle n_{A-\sigma}\rangle-\langle n_{B-\sigma}\rangle)^2+|t(\mathbf{k})|^2]^{1/2} \tag{2.50}$$

are spin dependent for the ferromagnet ($\langle n_{A\sigma}\rangle=\langle n_{B\sigma}\rangle=\langle n_{\sigma}\rangle$),

$$E_{\sigma p}^{(\mathrm{FM})}(\mathbf{k})=\eta_p(\mathbf{k})+U\langle n_{-\sigma}\rangle , \tag{2.51}$$

but spin independent in the case of an antiferromagnet

$$(\langle n_{A\sigma}\rangle=\langle n_{B-\sigma}\rangle) , \tag{2.52}$$

$$E_p^{(\mathrm{AFM})}(\mathbf{k})=\varepsilon(\mathbf{k})+\tfrac{1}{2}Un+p[\tfrac{1}{4}U^2m^2+|t(\mathbf{k})|^2]^{1/2} .$$

Here we have introduced the average particle number per site.

$$n=\sum_{\sigma}\langle n_{\alpha\sigma}\rangle , \tag{2.53}$$

which in any case is independent of sublattice index α.

The spectral weights in (2.49), however,

$$\gamma_{\sigma p}(\mathbf{k})=\frac{\varepsilon(\mathbf{k})+U\langle n_{A-\sigma}\rangle-E_{\sigma p}(\mathbf{k})}{E_{\sigma-p}(\mathbf{k})-E_{\sigma p}(\mathbf{k})} =1-\gamma_{\sigma-p}(\mathbf{k}) , \tag{2.54}$$

turn out to be spin independent for the ferromagnet,

$$\gamma_{\sigma p}^{(\mathrm{FM})}(\mathbf{k})=\tfrac{1}{2} , \tag{2.55}$$

but depend on spin in antiferromagnetic systems

$$\gamma_{\sigma p}^{(\mathrm{AFM})}(\mathbf{k})=\frac{1}{2}\left[1-z_\sigma p\frac{mU}{[U^2m^2+4|t(\mathbf{k})|^2]^{1/2}}\right] \tag{2.56}$$

(z_σ is a sign factor, $z_\uparrow=1$, $z_\downarrow=-1$).

The Stoner QDOS $\rho_{A\sigma}^{(S)}(\mathbf{k})$ is decisively influenced by the average particle number $\langle n_{\alpha-\sigma}\rangle$ and therewith by temperature T and band occupation $n(0\le n\le 2)$. $\langle n_{\alpha-\sigma}\rangle$ must be determined self-consistently via

$$\langle n_{\alpha-\sigma}\rangle=\int_{-\infty}^{+\infty} dE\, f_-(E)\rho_{\alpha-\sigma}^{(S)}(E) . \tag{2.57}$$

It turns out that the paramagnetic solution (PM),

$$\langle n_{\alpha\sigma}\rangle=\langle n_{\alpha-\sigma}\rangle , \tag{2.58}$$

exists for all parameter constellations. However, under certain conditions, concerning U, n, and T, additional ferro- and antiferromagnetic solutions appear. At $T=0$ the internal energy E_0 has to decide which solution is stable,

$$E_0=\langle H_S\rangle=\sum_{\mathbf{k},p,\sigma}E_{\sigma p}(\mathbf{k})f_-(E_{\sigma p}(\mathbf{k})) . \tag{2.59}$$

The corresponding $T=0$ phase diagram of the Stoner model is plotted in Fig. 1. For small band occupations n and not too high Coulomb interaction U only paramagnetism exists. For a fixed band filling n we find a critical $U_c^{\mathrm{FM}}(n)$, above which a ferromagnetic solution becomes possible and a critical $U_c^{\mathrm{AFM}}(n)$ for the antiferromagnetic counterpart. With increasing n towards the half-filled band ($n\to 1$), the critical U becomes smaller, where, however, $U_c^{\mathrm{FM}}(n)$ approaches a finite minimum value $U_{\min}$. For $U<U_{\min}=U_c^{\mathrm{FM}}(n=1)$, ferromagnetic solutions do not exist irrespective of n. Antiferromagnetism, however, appears in the half-filled band ($n=1$) even for $U=0^+$.

In wide regions of the (U,n) plane three mathematical solutions are simultaneously possible. Antiferromagnetism (AFM) and ferromagnetism (FM) are always stable against paramagnetism (PM). AFM dominates in a narrow tube around the $n=1$ axis.

Much can be learned from the quasiparticle density of states, which is plotted in Fig. 2 for a typical ferromagnetic situation. We recognize the well-known Stoner picture for band ferromagnetism, i.e., the exchange splitting into two spin-polarized subbands. They are nondeformed but rigidly shifted against one another by an energy amount of Um. The splitting is therefore temperature dependent, disappearing above T_C. The example in Fig. 2 shows a $T=0$ exchange shift of $Um=Un=2.8$ eV. Such a shift has to be removed at T_C. This is the reason for the unrealistic Curie temperature, predicted by the

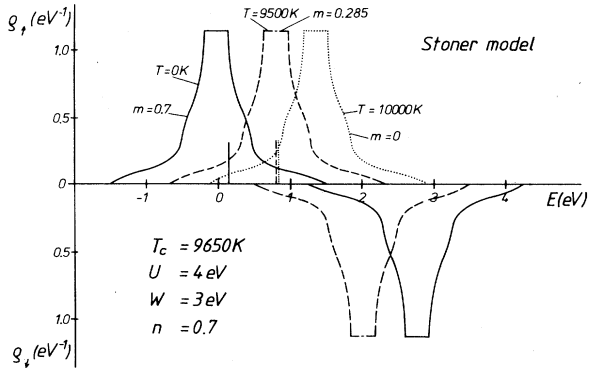

FIG. 2. Spin-dependent quasiparticle density of states $\rho_{\uparrow\downarrow}$ of the *ferromagnetic* Stoner model as function of energy for three different temperatures. Chosen parameters are indicated. The bars on the E axis mark the chemical potential $\mu=\mu(T,n)$.

Stoner model ($T_c=9650$ K). It is often claimed that the Stoner model reproduces the ground-state properties rather well. It is, however, completely overcharged to describe the correct temperature dependence of band ferromagnetism.

In Fig. 3 we have plotted the sublattice QDOS $\rho_{A\sigma}(E)$ for an antiferromagnetic system, using almost the same parameters as in Fig. 2. Below T_N both spin spectra are split into two subbands, where corresponding $\uparrow$ and $\downarrow$ subbands occupy exactly the same energy region but with different densities of states. This prevents the sublattice magnetization from being saturated even at $T=0$, a typical feature of each antiferromagnet. In the ferromagnetic case (Fig. 2) saturation is reached as soon as the lower edge of the $\downarrow$ subband lies above the Fermi energy. With increasing temperature the density of states of the low-energy $\downarrow$ subband grows up at cost of the $\uparrow$ subband leading therewith to a continuous decrease of the sublattice magnetization. Simultaneously the gap becomes smaller, disappearing for $T\geq T_N$. We see that the mechanism, which leads to a decrease of magnetization with increasing temperature, is different in ferromagnets and antiferromagnets. In ferromagnetic systems it is due to an increasing overlap of $\uparrow$ and $\downarrow$ subbands. In antiferromagnets it follows from a proper change of the QDOS.

Like T_C in Fig. 2 the Neel temperature T_N turns out to

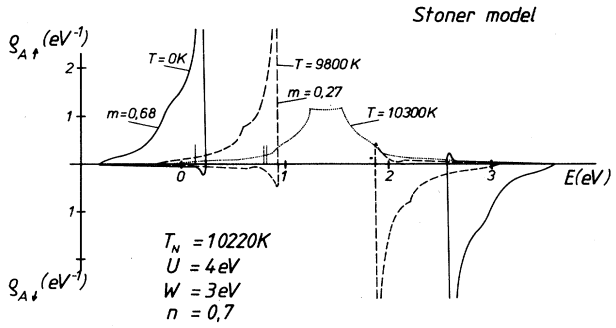

FIG. 3. The same as in Fig. 2, but for the sublattice QDOS $\rho_{A\uparrow\downarrow}$ of the *antiferromagnetic* Stoner model.

be extremely unrealistic, so that again the whole temperature behavior of the band antiferromagnet, as predicted by the Stoner model, must be questioned.

In many one-electron band-structure calculations based on density-functional theory, ferro- or antiferromagnetism is implemented by an ansatz, which corresponds more or less to the Stoner concept. As we shall explain in detail in connection with our own propsal for the T dependence of the QDOS, we consider the Stoner ansatz as rather misleading.

III. SELF-CONSISTENT MOMENT METHOD

A. Spectral-density approach

As already mentioned in Sec. II A the decisive quantity of our procedure is the one-electron spectral density $S^{\alpha\beta}_{\mathbf{k}\sigma}(E)$, defined in Eq. (2.14), from which we can derive all information we are interested in. The goal is therefore to find a physically reasonable approach to this fundamental function. Our spectral-density approach (SDA) consists of two steps.[41] First we try to find out the very general structure of the spectral density, guided by some arguments from exactly known limiting cases, series expansions, spectral decompositions, or by other plausible physical hints. These considerations should result in a mathematical ansatz for the spectral density, which shall contain some free parameters. In the second step we then fit these free parameters by equating a sufficient number of so-called spectral moments, which can exactly be calculated independently of the required spectral density. This method has succesfully been applied in several papers to different models.[41,43,44]

The crucial point is the choice of a physically reasonable ansatz for the spectral density, the further procedure then does not need any other approximation.

The natural starting point is the spectral density $A_{\mathbf{k}\sigma p}(E)$, defined in (2.36) because it is built up by the operators $d_{\mathbf{k}\sigma p}$ and $d^{\dagger}_{\mathbf{k}\sigma p}$, which diagonalize the free part H_0 of the model Hamiltonian (2.22). The spectral decomposition of this fundamental function reads as,

$$A_{\mathbf{k}\sigma p}(E)=\frac{\hbar}{\Xi}\sum_{n,m} e^{-\beta E_n}|\langle E_n|d^{\dagger}_{\mathbf{k}\sigma p}|E_m\rangle|^2(1+e^{\beta E}) \times\delta(E-(E_n-E_m))\ . \tag{3.1}$$

Ξ is the grand canonical partition function. $|E_m\rangle$ is an N-particle eigenstate, an $|E_n\rangle$ an $(N+1)$ particle eigenstate of the Hamiltonian H. E_n, E_m are the corresponding eigenenergies. The spectral density thus represents a linear combination of positively weighted δ functions, the arguments of which contain just the excitation energies which must be brought up for adding an additional $(\mathbf{k},p,\sigma)$ electron to the N-particle system. It is easy to show that in the zero-band width limit ($W\to 0$) the spectral density consists of two δ peaks, positioned at $E_n-E_m=T_0$ and $E_n-E_m=T_0+U$, respectively. In the $W\to 0$ case the electrons are strictly localized. To add a further electron to the system therefore requires the energy T_0, if we place it on an empty site, and the energy T_0+U, if there is already another electron with opposite

spin present. For finite bandwidth ($W \neq 0$) we have to take into consideration the itineracy of the band electrons. As soon as we bring an additional $(\mathbf{k},p,\sigma)$ electron into the system, the hopping of the already present electrons may lead to a change in the number of doubly occupied sites as a response to the arrival of the $(N+1)$ electron. As a consequence of such electron correlations, we have, therefore, to expect satellite peaks in the spectral density close to the energies $E_d^{(+)}=T_0+(d+1)U$ and $E_d^{(-)}=T_0-dU\,(d=1,2,\ldots)$. Furthermore, lifetime effects will smear out the peaks in the spectral density. The probability for the appearance of satellite peaks is surely greater the more likely the electron hopping, and smaller the larger the Coulomb matrix element U. It has been shown by Harris and Lange[45] that the weights of the peaks at $E_1^{(\mp)}$, which are located next to the main peaks at T_0 and T_0+U, scale with $(W/U)^4$. The weights of the peaks at $E_{d>1}^{(\mp)}$ are proportional to even higher powers of W/U. We therefore believe that the following ansatz is physically reasonable, at least for not too weak electron correlations:

$$A_{\mathbf{k}\sigma p}(E)=\hbar\sum_{j=1}^{2}\alpha_{j\sigma p}(\mathbf{k})\delta(E-E_{j\sigma p}(\mathbf{k}))\ . \tag{3.2}$$

The spectral weights $\alpha_{j\sigma p}(\mathbf{k})$ and the quasiparticle energies $E_{j\sigma p}(\mathbf{k})$ are for the moment unknown parameters, which will be determined by equating exactly calculated spectral moments. We consider the $E_{j\sigma p}(\mathbf{k})$ to be real quantities, neglecting therewith damping effects.

The spectral decomposition of the "mixed" spectral density $D_{\mathbf{k}\sigma}^{(p,-p)}(E)$, defined in (2.37) reads as

$$D_{\mathbf{k}\sigma}^{(p,-p)}(E)=\frac{\hbar}{\Xi}\sum_{n,m}e^{-\beta E_n}\{\langle E_n|d_{\mathbf{k}\sigma-p}^{\dagger}|E_m\rangle\langle E_m|d_{\mathbf{k}\sigma p}|E_n\rangle\delta(E-(E_n-E_m))$$
$$+\langle E_n|d_{\mathbf{k}\sigma p}|E_r\rangle\langle E_r|d_{\mathbf{k}\sigma-p}^{\dagger}|E_n\rangle\delta(E-(E_r-E_n))\}\ . \tag{3.3}$$

$|E_r\rangle$ is now an $(N+2)$-particle eigenstate of the model Hamiltonian. The other symbols have exactly the same meaning as in (3.1). First we have to conclude from (3.3) that there is no real p dependence,

$$D_{\mathbf{k}\sigma}^{(+,-)}(E)\equiv D_{\mathbf{k}\sigma}^{(-,+)}(E)\equiv D_{\mathbf{k}\sigma}(E)\ . \tag{3.4}$$

Furthermore, by the same philosophy which led to the ansatz (3.2), we are now obliged to accept the following four-pole ansatz for the mixed spectral density:

$$D_{\mathbf{k}\sigma}(E)=\hbar\sum_{j=1}^{2}\sum_{p=\mp}\beta_{j\sigma p}(\mathbf{k})\delta(E-E_{j\sigma p}(\mathbf{k}))\ . \tag{3.5}$$

The quasiparticle energies are the same as in (3.2).

B. Spectral moments

The spectral moments have to be calculated with the model Hamiltonian (2.5). We, therefore, discuss first the moments of the spectral density $S_{ij\sigma}^{\alpha\beta}(E)$, introduced in (2.15). The crucial point is that there are two equivalent expressions for the moments,

$$M_{\mathbf{k}\sigma}^{(n)}(\alpha,\beta)=\frac{1}{N}\sum_{i,j}e^{-\mathbf{k}\cdot(\mathbf{R}_i-\mathbf{R}_j)}M_{ij\sigma}^{(n)}\ . \tag{3.6}$$

The one reveals the connection with the spectral density,

$$M_{\mathbf{k}\sigma}^{(n)}(\alpha,\beta)=\int_{-\infty}^{+\infty}dE\,E^nS_{\mathbf{k}\sigma}^{\alpha\beta}(E),\quad n=0,1,2,\ldots\ . \tag{3.7}$$

while the other allows the determination of the moments *independently* of the spectral density,

$$M_{ij\sigma}^{(n)}(\alpha,\beta)=\langle[[\ldots,[\underbrace{[c_{i\alpha\sigma},H]_-,H]_-,\ldots,H}_{r\text{-fold commutator}}]_-,[H,\ldots,[\underbrace{H,[H,c_{j\beta\sigma}^{\dagger}]_-]_-,\ldots,]_-}_{(n-r)\text{-fold commutator}}]_+\rangle\ . \tag{3.8}$$

$[,]_-$ denotes the commutator, $[,]_+$ the anticommutator, and $\langle\ldots\rangle$ the thermodynamic average, r is an integer between 0 and n. Tedious but straightforward calculations yield for the first four moments,

$$M_{\mathbf{k}\sigma}^{(0)}(\alpha,\beta)=\delta_{\alpha\beta}\ , \tag{3.9}$$

$$M_{\mathbf{k}\sigma}^{(1)}(\alpha,\beta)=\varepsilon_{\alpha\beta}(\mathbf{k})+\delta_{\alpha\beta}U\langle n_{\alpha-\sigma}\rangle\ , \tag{3.10}$$

$$M_{\mathbf{k}\sigma}^{(2)}(\alpha,\beta)=\sum_{\gamma}\varepsilon_{\alpha\gamma}(\mathbf{k})\varepsilon_{\gamma\beta}(\mathbf{k})+U\varepsilon_{\alpha\beta}(\mathbf{k})(\langle n_{\alpha-\sigma}\rangle+\langle n_{\beta-\sigma}\rangle)+U^2\delta_{\alpha\beta}\langle n_{\alpha-\sigma}\rangle\ , \tag{3.11}$$

$$M_{\mathbf{k}\sigma}^{(3)}(\alpha,\beta)=\sum_{\gamma,\delta}\varepsilon_{\alpha\gamma}(\mathbf{k})\varepsilon_{\gamma\delta}(\mathbf{k})\varepsilon_{\delta\beta}(\mathbf{k})+U\sum_{\gamma}\varepsilon_{\alpha\gamma}(\mathbf{k})\varepsilon_{\gamma\beta}(\mathbf{k})(\langle n_{\alpha-\sigma}\rangle+\langle n_{\beta-\sigma}\rangle+\langle n_{\gamma-\sigma}\rangle)$$
$$+U^2[\varepsilon_{\alpha\beta}(\mathbf{k})(\langle n_{\alpha-\sigma}\rangle+\langle n_{\beta-\sigma}\rangle+\langle n_{\alpha-\sigma}\rangle\langle n_{\beta-\sigma}\rangle)+B_{\mathbf{k}-\sigma}^{\alpha\beta}]+U^3\delta_{\alpha\beta}\langle n_{\alpha-\sigma}\rangle\ . \tag{3.12}$$

Here we have introduced the band correction

$$B^{\alpha\beta}_{\mathbf{k}\sigma}=B^{\alpha\beta}_{W;\sigma}(\mathbf{k})+\delta_{\alpha\beta}B^{\alpha}_{S;\sigma} \ . \tag{3.13}$$

Of decisive importance concerning the possibility of spontaneous magnetic order is the spin-dependent band shift $B^{\alpha\beta}_{S;\sigma}$,

$$B^{\alpha}_{S:\sigma}=\frac{1}{N}\sum_{i,j,\gamma} T^{\alpha\gamma}_{ij}\langle c^{\dagger}_{i\alpha\sigma}c_{j\gamma\sigma}(2n_{i\alpha-\sigma}-1)\rangle \ . \tag{3.14}$$

We demonstrate in the next section how $B^{\alpha}_{S;\sigma}$ may be expressed by the one-electron spectral density $S^{\alpha\beta}_{\mathbf{k}\sigma}(E)$, although it consists of higher correlation functions.

The second term in the band correction turns out to be of minor importance

$$B^{\alpha\beta}_{W;\sigma}(\mathbf{k})=\frac{1}{N}\sum_{i,j} T^{\alpha\beta}_{ij}e^{-i\mathbf{k}\cdot(\mathbf{R}_i-\mathbf{R}_j)}(\langle n_{i\alpha\sigma}n_{j\beta\sigma}\rangle-\langle n_{\alpha\sigma}\rangle\langle n_{\beta\sigma}\rangle-\langle c^{\dagger}_{j\beta\sigma}c^{\dagger}_{j\beta-\sigma}c_{i\alpha-\sigma}c_{i\alpha\sigma}\rangle-\langle c^{\dagger}_{j\beta-\sigma}c^{\dagger}_{i\alpha\sigma}c_{j\beta\sigma}c_{i\alpha-\sigma}\rangle) \ . \tag{3.15}$$

The first two terms represent the density correlation between two sites, which obviously disappears in a mean-field approach. The third term characterize double hopping from site to site, vanishing in the strong-coupling regime ($U\gg W, n\leq 1$), when double occupancies of lattice sites become rather unlikely. The last term in (3.15) expresses spin exchange between electrons on different sites, where spin exchange as well as double hopping are unaffected by a spin reversal ($\sigma \Longleftrightarrow -\sigma$). They are, therefore, not that important with respect to the possibility of ferro- or antiferromagnetism. From these reasons we simplify the third spectral moment by

$$B^{\alpha\beta}_{W;\sigma}(\mathbf{k})\simeq 0 \ . \tag{3.16}$$

For the spectral densities $A_{\mathbf{k}\sigma p}(E)$ and $D_{\mathbf{k}\sigma}(E)$, which contain the unknown parameters, we need the moments in special combinations. First we recognize that

$$p[t^*(\mathbf{k})/|t(\mathbf{k})|]M^{(n)}_{\mathbf{k}\sigma}(A,B)=p[t(\mathbf{k})/|t(\mathbf{k})|]M^{(n)}_{\mathbf{k}\sigma}(B,A) \ . \tag{3.17}$$

Using this and Eqs. (2.32) and (2.33) in (2.36) and (2.37) we find the following connections of $A_{\mathbf{k}\sigma p}(E)$ and $D_{\mathbf{k}\sigma}(E)$ with $S^{\alpha\beta}_{\mathbf{k}\sigma}(E)$:

$$A_{\mathbf{k}\sigma p}(E)=\tfrac{1}{2}\sum_{\alpha}^{A,B} S^{\alpha\alpha}_{\mathbf{k}\sigma}(E)+p[t^*(\mathbf{k})/|t(\mathbf{k})|]S^{AB}_{\mathbf{k}\sigma}(E) \ , \tag{3.18}$$

$$D_{\mathbf{k}\sigma}(E)=\tfrac{1}{2}[S^{AA}_{\mathbf{k}\sigma}(E)-S^{BB}_{\mathbf{k}\sigma}(E)] \ . \tag{3.19}$$

For the determination of the four free parameters in the spectral density $A_{\mathbf{k}\sigma p}(E)$, we need the following moment combination:

$$\mu^{(n)}_{\mathbf{k}\sigma p}=\tfrac{1}{2}\sum_{\alpha}^{A,B} M^{(n)}_{\mathbf{k}\sigma}(\alpha,\alpha)+p[t^*(\mathbf{k})/|t(\mathbf{k})|]M^{(n)}_{\mathbf{k}\sigma}(A,B) \ , \tag{3.20}$$

while the mixed spectral density is fixed by

$$m^{(n)}_{\mathbf{k}\sigma}=\tfrac{1}{2}[M^{(n)}_{\mathbf{k}\sigma}(A,A)-M^{(n)}_{\mathbf{k}\sigma}(B,B)] \ . \tag{3.21}$$

In order to get a closed system of equations we have finally to express the spin-dependent band shift $B^{\alpha}_{S:\sigma}$ by the spectral densities $A_{\mathbf{k}\sigma p}(E)$ and $D_{\mathbf{k}\sigma}(E)$. Surprisingly, this is possible, although $B^{\alpha}_{S;-\sigma}$ is built up by higher correlation functions.

C. Spin-dependent band shift

According to Eq. (3.14) the band shift $B^{\alpha}_{S;-\sigma}$ is mainly determined by the correlation function

$$\langle c^{\dagger}_{i\alpha\sigma}c_{j\gamma\sigma}n_{i\alpha-\sigma}\rangle \ ,$$

which we evaluate by the following procedure. First we calculate with (2.5) the commutator

$$[H,c^{\dagger}_{i\alpha-\sigma}]_-=\sum_{m,\gamma} T^{\gamma\alpha}_{mi}c^{\dagger}_{m\gamma-\sigma}+Un_{i\alpha\sigma}c^{\dagger}_{i\alpha-\sigma} \ . \tag{3.22}$$

Multiplying this expression from the right by $c_{j\beta-\sigma}$ and then averaging yields

$$U\langle n_{i\alpha\sigma}c^{\dagger}_{i\alpha-\sigma}c_{j\beta-\sigma}\rangle=\langle[H,c^{\dagger}_{i,\alpha-\sigma}]_-c_{j\beta-\sigma}\rangle-\sum_{m,\gamma} T^{\gamma\alpha}_{mi}\langle c^{\dagger}_{m\gamma-\sigma}c_{j\beta-\sigma}\rangle \ . \tag{3.23}$$

We now define a "higher" spectral density

$$\hat{S}_{ij-\sigma}^{\alpha\beta}(t,t')=\frac{1}{2\pi}\langle[c_{j\beta-\sigma}(t),[H,c_{i\alpha-\sigma}^{\dagger}]_{-}(t')]_{+}\rangle \tag{3.24}$$

and use the general spectral theorem[42] to get

$$\langle[H,c_{i\alpha-\sigma}^{\dagger}]_{-}c_{j\beta-\sigma}\rangle=\frac{1}{\hbar}\int_{-\infty}^{+\infty}dE\,f_{-}(E)\int_{-\infty}^{+\infty}d(t-t')e^{i/\hbar E(t-t')}\hat{S}_{ij-\sigma}^{\alpha\beta}(t-t')\ . \tag{3.25}$$

$\hat{S}_{ij\sigma}^{\alpha\beta}$ can be expressed in terms of the one-electron spectral density $S_{ij\sigma}^{\alpha\beta}$

$$\begin{aligned}\hat{S}_{ij-\sigma}^{\alpha\beta}(t-t')&=-\frac{i}{\hbar}\frac{\partial}{\partial t'}\frac{1}{2\pi}\langle[c_{j\beta-\sigma}(t),c_{i\alpha-\sigma}^{\dagger}(t')]_{+}\rangle\\&=\frac{1}{2\pi\hbar}\int_{-\infty}^{+\infty}dE'\,E'e^{-i/\hbar E'(t-t')}S_{ji-\sigma}^{\beta\alpha}(E')\ .\end{aligned} \tag{3.26}$$

Combining (3.25) and (3.26) leads to

$$\langle[H,c_{i\alpha-\sigma}^{\dagger}]c_{j\beta-\sigma}\rangle=\frac{1}{\hbar}\int_{-\infty}^{+\infty}dE\,f_{-}(E)ES_{ji-\sigma}^{\beta\alpha}(E)\ . \tag{3.27}$$

Applying once more the spectral theorem, but now to the one-electron spectral density, we get

$$\langle c_{m\gamma-\sigma}^{\dagger}c_{j\beta-\sigma}\rangle=\frac{1}{\hbar}\int_{-\infty}^{+\infty}dE\,f_{-}(E)S_{jm-\sigma}^{\beta\gamma}(E)\ . \tag{3.28}$$

We insert (3.27) and (3.28) into (3.23)

$$\langle n_{i\alpha\sigma}c_{i\alpha-\sigma}^{\dagger}c_{j\beta-\sigma}\rangle=\frac{1}{U}\frac{1}{\hbar N}\sum_{\mathbf{k},\gamma}e^{i\mathbf{k}\cdot(\mathbf{R}_j-\mathbf{R}_i)}\int_{-\infty}^{+\infty}dE\,f_{-}(E)[E\delta_{\gamma\alpha}-\varepsilon_{\gamma\alpha}(\mathbf{k})]S_{\mathbf{k}-\sigma}^{\beta\gamma}(E)\ . \tag{3.29}$$

For the band shift (3.29) we need,

$$\frac{1}{N}\sum_{i,j,\beta}T_{ij}^{\alpha\beta}\langle n_{i\alpha\sigma}c_{i\alpha-\sigma}^{\dagger}c_{j\beta-\sigma}\rangle=\frac{1}{U\hbar}\frac{1}{N}\sum_{\mathbf{k},\beta,\gamma}\varepsilon_{\alpha\beta}(\mathbf{k})\int_{-\infty}^{+\infty}dE\,f_{-}(E)[E\delta_{\gamma\alpha}-\varepsilon_{\gamma\alpha}(\mathbf{k})]S_{\mathbf{k}-\sigma}^{\beta\gamma}(E) \tag{3.30}$$

and

$$\frac{1}{N}\sum_{i,j,\beta}T_{ij}^{\alpha\beta}\langle c_{i\alpha-\sigma}^{\dagger}c_{j\beta-\sigma}\rangle=\frac{1}{\hbar N}\sum_{\mathbf{k},\beta}\varepsilon_{\alpha\beta}(\mathbf{k})\int_{-\infty}^{+\infty}dE\,f_{-}(E)S_{\mathbf{k}-\sigma}^{\beta\alpha}(E)\ . \tag{3.31}$$

If we replace the spectral densities $S_{\mathbf{k}\sigma}^{\alpha\beta}(E)$ by $A_{\mathbf{k}\sigma p}(E)$ and $D_{\mathbf{k}\sigma}(E)$ with the aid of Eqs. (2.38)–(2.41) and (3.4), exploiting also the ansatz (3.2) and (3.5), then we finally get with (3.30) and (3.31) in (3.13) the spin-dependent band shift,

$$B_{S;-\sigma}^{A}=\tfrac{1}{2}[Q_{-\sigma}+(\langle n_{A-\sigma}\rangle-\langle n_{B-\sigma}\rangle)B_{-\sigma}]\ , \tag{3.32}$$

$$Q_{-\sigma}=\frac{1}{N}\sum_{\mathbf{k}}\sum_{p,j}\alpha_{j-\sigma p}(\mathbf{k})f_{-}(E_{j-\sigma p})\eta_{p}(\mathbf{k})\left[\left[\frac{2}{U}(E_{j-\sigma p}(\mathbf{k})-\eta_{p}(\mathbf{k})\right]-1\right]\ , \tag{3.33}$$

$$\begin{aligned}B_{-\sigma}=&\frac{1}{(\langle n_{A-\sigma}\rangle-\langle n_{B-\sigma}\rangle)}\frac{1}{N}\\&\times\sum_{\mathbf{k}}\sum_{p,j}\beta_{j-\sigma p}(\mathbf{k})f_{-}(E_{j-\sigma p})\left\{\varepsilon(\mathbf{k})\left[\left[\frac{2}{U}(E_{j-\sigma p}(\mathbf{k})-\varepsilon(\mathbf{k})\right]-1\right]+\frac{2}{U}|t(\mathbf{k})|^{2}\right\}\ .\end{aligned} \tag{3.34}$$

This completes our general theory, because now we have a closed system of equations, which can be solved self-consistently for the particle numbers $\langle n_{\alpha\uparrow}\rangle$, $\langle n_{\alpha\downarrow}\rangle$.

We mention in passing that (3.29) together with (3.31) allows the determination of the internal energy $E_0=\langle H\rangle$,

$$E_0=\langle H\rangle=\frac{1}{2\hbar}\sum_{\mathbf{k},\sigma,\alpha,\beta}\int_{-\infty}^{+\infty}dE\,f_{-}(E)[E\delta_{\alpha\beta}+\varepsilon_{\alpha\beta}(\mathbf{k})]S_{\mathbf{k}\sigma}^{\beta\alpha}(E)\ . \tag{3.35}$$

We need this expression for testing the relative stability of different magnetic solutions.

D. Ferromagnetic solutions

The ferromagnet is characterized by two completely equivalent sublattices A and B. So we can assume

$$\langle n_{A\sigma}\rangle=\langle n_{B\sigma}\rangle=\langle n_{\sigma}\rangle\ , \tag{3.36}$$

$$B_{S;\sigma}^{A}=B_{S;\sigma}^{B}=B_{S;\sigma}\ . \tag{3.37}$$

According to (3.21) all moments $m_{\mathbf{k}\sigma}^{(n)}$ vanish identically. That means for the mixed spectral density $D_{\mathbf{k}\sigma}(E)$ in the case of the ferromagnet,

$$D_{\mathbf{k}\sigma}(E)\equiv 0 \Longleftrightarrow \beta_{j\sigma p}\equiv 0 \ . \tag{3.38}$$

The band shift (3.32) which regulates the appearance of ferromagnetism simplifies with (3.38) to

$$\begin{aligned} B_{S;-\sigma} &= \frac{1}{2N}\sum_{\mathbf{k}}\sum_{p,j}\alpha_{j-\sigma p}(\mathbf{k}) f_{-}(E_{j-\sigma p})\eta_p(\mathbf{k}) \\ &\quad\times\left[\frac{2}{U}[E_{j-\sigma p}(\mathbf{k})-\eta_p(\mathbf{k})]-1\right] \\ &\equiv \langle n_{-\sigma}\rangle(1-\langle n_{-\sigma}\rangle)b_{-\sigma} \ . \end{aligned} \tag{3.39}$$

The four unknown quantities $\alpha_{1,2,\sigma p}, E_{1,2\sigma p}$ in the ansatz (3.7) for the spectral density $A_{\mathbf{k}\sigma p}(E)$ are determined by equating the first four μ moments (3.20),

$$\mu^{(n)}_{\mathbf{k}\sigma p} = \int_{-\infty}^{+\infty} dE\, E^n A_{\mathbf{k}\sigma p}(E) \ . \tag{3.40}$$

If we write for the quasiparticle energies $E_{j\sigma p}$,

$$E_{j\sigma p}(\mathbf{k}) = H_{\sigma p}(\mathbf{k}) + (-1)^j K_{\sigma p}(\mathbf{k}) \ , \tag{3.41}$$

then it follows from (3.40) and (3.20) and (3.9)–(3.12)

$$H_{\sigma p}(\mathbf{k}) = \tfrac{1}{2}[U+\eta_p(\mathbf{k})+b_{-\sigma}] \ , \tag{3.42}$$

$$\begin{aligned} K_{\sigma p}(\mathbf{k}) &= \tfrac{1}{2}\{[U-\eta_p(\mathbf{k})+b_{-\sigma}]^2 \\ &\quad +4U\langle n_{-\sigma}\rangle[\eta_p(\mathbf{k})-b_{-\sigma}]\}^{1/2} \ . \end{aligned} \tag{3.43}$$

The spectral weights turn out to be

$$\begin{aligned} \alpha_{1\sigma p}(\mathbf{k}) &= \frac{E_{2\sigma p}(\mathbf{k})-\eta_p(\mathbf{k})-U\langle n_{-\sigma}\rangle}{E_{2\sigma p}(\mathbf{k})-E_{1\sigma p}(\mathbf{k})} \\ &= 1-\alpha_{2\sigma p}(\mathbf{k}) \ . \end{aligned} \tag{3.44}$$

By use of the quasiparticle density of states

$$\begin{aligned} \rho_\sigma(E) &\equiv \rho_{A\sigma}(E) \\ &= \rho_{B\sigma}(E) \\ &= \frac{1}{2N}\sum_{\mathbf{k}}\sum_{p,j}\alpha_{j\sigma p}(\mathbf{k})\delta(E-E_{j\sigma p}) \ , \end{aligned} \tag{3.45}$$

we finally get the average number of σ electrons per site:

$$\langle n_\sigma\rangle = \int_{-\infty}^{+\infty} dE\, f_{-}(E)\rho_\sigma(E) \ . \tag{3.46}$$

The system of equations (3.39)–(3.46) can be solved self-consistently for a given set of parameters. Results are presented in Sec. IV.

E. Antiferromagnetic solution

The two sublattices A and B of the antiferromagnet are not equivalent, obeying, however, the obvious spin symmetry

$$(A,\sigma)\hat{=}(B,-\sigma) \ . \tag{3.47}$$

That means, e.g.,

$$\langle n_{A\sigma}\rangle = \langle n_{B-\sigma}\rangle \ , \quad B^A_{S;\sigma} = B^B_{S;-\sigma} \ . \tag{3.48}$$

Let us define the sublattice magnetization m as

$$m = z_\sigma(\langle n_{A\sigma}\rangle - \langle n_{A-\sigma}\rangle) = -z_\sigma(\langle n_{B\sigma}\rangle - \langle n_{B-\sigma}\rangle) \ . \tag{3.49}$$

The μ moments (3.20) are now spin independent, a property which is directly referred to the quasiparticle energies E_{jp} and spectral weights α_{jp}

$$E_{jp}(\mathbf{k}) = H_p(\mathbf{k}) + (-1)^j K_p(\mathbf{k}) \ , \tag{3.50}$$

$$H_p(\mathbf{k}) = \tfrac{1}{2}[U+\eta_p(\mathbf{k})+b_p(\mathbf{k})] \ , \tag{3.51}$$

$$\begin{aligned} K_p(\mathbf{k}) &= \tfrac{1}{2}\{[U(1-n)-\eta_p(\mathbf{k})+b_p(\mathbf{k})]^2 \\ &\quad +U^2 n(2-n)\}^{1/2} \ . \end{aligned} \tag{3.52}$$

Here we have defined,

$$b_p(\mathbf{k}) = \frac{Q+\frac{1}{2}m^2\eta_{-p}(\mathbf{k})}{n(1-n/2)} \ . \tag{3.53}$$

The quantity Q is the antiferromagnetic version of (3.33),

$$\begin{aligned} Q &= \frac{1}{N}\sum_{\mathbf{k}}\sum_{j,p}\alpha_{jp}(\mathbf{k}) f_{-}(E_{jp})\eta_p(\mathbf{k}) \\ &\quad\times\left[\frac{2}{U}[E_{jp}(\mathbf{k})-\eta_p(\mathbf{k})]-1\right] \ . \end{aligned} \tag{3.54}$$

The spectral weights α_{jp} are formally very similar to (3.44)

$$\begin{aligned} \alpha_{1p}(\mathbf{k}) &= \frac{E_{2p}(\mathbf{k})-\eta_p(\mathbf{k})-\frac{1}{2}Un}{E_{2p}(\mathbf{k})-E_{1p}(\mathbf{k})} \\ &= 1-\alpha_{2p}(\mathbf{k}) \ . \end{aligned} \tag{3.55}$$

The spin independence of the quasiparticle energies $E_{jp}(\mathbf{k})$ makes clear that both spin spectra occupy exactly the same energy region. Antiferromagnetic moment order must therefore be a density-of-states effect. Contrary to the ferromagnet the mixed spectral density $D_{\mathbf{k}\sigma}(E)$ is now unequal zero and of decisive importance for a spontaneous moment ordering. We determine the still unknown coefficients $\beta_{j\sigma p}$ in the ansatz (3.5) by equating the first four moments $m^{(n)}_{\mathbf{k}\sigma}$ (3.21). After straightforward manipulations one gets

$$\beta_{j\sigma p} = -\tfrac{1}{2}z_\sigma m U q_{jp}(\mathbf{k}) \ , \tag{3.56}$$

$$\begin{aligned} q_{jp}(\mathbf{k}) &= \frac{1}{W_{jp}}\{U^2+U[B+(2+n)\varepsilon(\mathbf{k})-X_{jp}] \\ &\quad +3\varepsilon^2(\mathbf{k})+|t(\mathbf{k})|^2-2\varepsilon(\mathbf{k})X_{jp}+V_{jp}\} \ , \end{aligned} \tag{3.57}$$

$$X_{jp} = 2(H_+ + H_-) - E_{jp} \ , \tag{3.58}$$

$$W_{jp} = \prod_{(j',p')}^{\neq(j,p)}(E_{jp}-E_{j'p'}) \ , \tag{3.59}$$

$$V_{jp} = 2H_+H_- + 2(-1)^{j-1}K_pH_{-p} + H^2_{-p} - K^2_{-p} \ . \tag{3.60}$$

The quantity B is the antiferromagnetic version of (3.34).

The sublattice density of states $\rho_{A\sigma}(E)$ consists of two

parts, one is spin dependent, the other is not

$$\rho_{A\sigma}(E)=\frac{1}{2N}\sum_{\mathbf{k}}\sum_{j,p}[\alpha_{jp}(\mathbf{k})-z_\sigma mUq_{jp}(\mathbf{k})]\delta(E-E_{jp}(\mathbf{k}))$$
$$=\rho_{B-\sigma}(E)\ . \tag{3.61}$$

The average number of σ electrons per site in the sublattice A is then given by

$$\langle n_{A\sigma}\rangle=\frac{1}{2N}\sum_{\mathbf{k}}\sum_{j,p}f_-(E_{jp})[\alpha_{jp}(\mathbf{k})-z_\sigma mUq_{jp}(\mathbf{k})]\ . \tag{3.62}$$

The total number n per site is, therefore, mainly determined by the spectral weights α_{jp},

$$n=\sum_\sigma\langle n_{\alpha\sigma}\rangle=\frac{1}{N}\sum_{\mathbf{k}}\sum_{j,p}\alpha_{jp}(\mathbf{k})f_-(E_{jp}(\mathbf{k}))\ , \tag{3.63}$$

while the sublattice magnetization m is predominantly influenced by the coefficients of the "mixed" spectral density $D_{\mathbf{k}\sigma}(E)$,

$$m=-mU\frac{1}{N}\sum_{\mathbf{k}}\sum_{j,p}q_{jp}(\mathbf{k})f_-(E_{jp}(\mathbf{k}))\ . \tag{3.64}$$

Equations (3.50)–(3.64) represent a closed system, which can be solved self-consistently. We discuss the results in the next section.

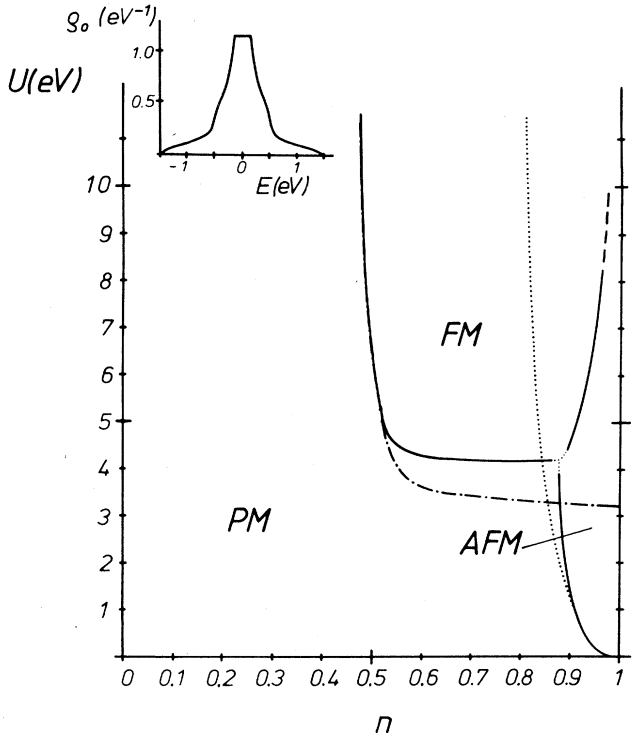

FIG. 4. As in Fig. 1, the $T=0$ phase diagram in terms of Coulomb interation U and band occupation n, but now as it results from our spectral-density approach (SDA) to the Hubbard model.

IV. DISCUSSION OF THE RESULTS

A. Magnetic phase diagram

We have evaluated our theory for a Bloch density of states $\rho_0(E)$ as defined in (2.44)–(2.46). $\rho_0(E)$ is plotted as the insert in Figs. 1 and 4. Figure 4 shows the magnetic phase diagram for $T=0$ in terms of the Coulomb interaction U and the band occupation n. We restrict the representation to $0\le n\le 1$. The region $1\le n\le 2$ follows directly by reflection on the $n=1$ axis because of particle-hole symmetry.

We recognize a minimum band occupation $n_0\simeq 0.44$, below which magnetic order is impossible. For $n\ge n_0$ ferromagnetic solutions appear, provided U exceeds a critical value $U_c^{\mathrm{FM}}(n)$. For $0.5\le n\le 1$ this critical value is almost constant, slightly greater than the Bloch band width W. For $U<W$ the system cannot order ferromagnetically irrespective of the band occupation n. Antiferromagnetism becomes possible for $n\ge 0.77$, where again U has to exceed a critical value $U_c^{\mathrm{AFM}}(n)$, which, however, decreases continuously down to zero for $n\to 1$. In certain (n,U) regions our theory has more than one mathematical solution; the paramagnetic one, e.g., exists for all n. At $T=0$ the internal energy $E=\langle H\rangle$, calculated with (3.35) decides, which solution is stable. In a narrow n region around the half-filled band ($n=1$) antiferromagnetism dominates where this region is broadest for $U\simeq W$, obviously the most convenient parameter constellation for an antiferromagnetic moment ordering. For larger U the phase line between antiferro- and ferromagnetism approaches more and more the $n=1$ axis. The same holds for smaller U for the phase line between antiferro- and paramagnetism, which runs into $n=1$ for $U\to 0^+$. Very recently Zhao *et al.*[33] have calculated a magnetic phase diagram by use of a perturbational method, which in the strong-correlation regime ($W/U\ll 1$) is qualitatively very similar to our result. They confirm, e.g., the existence of a critical band occupation n_0, below which collective magnetic order is impossible. On the other hand, in the Stoner model a critical n value does not appear (Fig. 1). In the weak-correlation regime ($U\ll W$), however, there is a certain resemblance of our phase diagram in Fig. 4 to the Stoner result in Fig. 1. Generally the Stoner model overestimates the possiblility of spontaneous magnetization.

A controversial discussion may arise from the observation that our approach predicts that the antiferromagnetic solution at $T=0$ remains stable along the $n=1$ line down to $U=0^+$. This contradicts some previous works[46–48] based on Gutzwiller's variational approach, which point to a critical $U_c>0$ for the antiferromagnet, too. Our spectral-density approach uses, in principle, only one assumption, which concerns the general structure of the one-electron spectral density. This is just the two-pole ansatz (3.2). Further evaluation is rigorous. Equation (3.2) is surely justified for large U, say $U>W$. We consider it, however, plausible for moderate and even for small U, too, at least as long as we are not interested special life-time effects. We have, of course, to admit that

our ansatz cannot be justified in the weak-coupling regime so convincingly as for $U > W$. For weak correlation ($U \ll W$) the Hartree-Fock approach (Stoner model), however, should be reasonable. The resemblance of the phase diagram in Fig. 4 with that in Fig. 1 in the weak-coupling regime therefore strongly supports the assumption that the SDA works well in the entire (U,n) region.

On the other hand, the various theories, which start from an extension of Gutzwiller's variational method to the antiferromagnetic state, come to partially contradicting statements about the $U \ll W$ regime, because they use different additional approximations. In Refs. 46–48 a critical U_c is found, below which antiferromagnetism becomes unstable against paramagnetism, while the Gutzwiller-type variational approach of Kakehashi and Fulde[29] is in complete agreement with our conclusions in Fig. 4 (see also Fig. 1 in Ref. 31). The approximations used by Florencio and Chao in Ref. 48, e.g., are so restrictive that the authors themselves point out that the real criterion for antiferromagnetism should be less stringent than what is predicted by their own theory.

B. Spontaneous magnetization

The self-consistently calculated sublattice magnetization m, which in the case of a ferromagnet (FM) is, of course, identical to the total magnetization, shows a strong T and n dependence. Both are direct consequences of the respective behavior of the quasiparticle density of states (QDOS) discussed in detail in Sec. IV D. In Fig. 5 we have plotted the n dependence of the $T=0$ magnetization for a ferromagnet, and in Fig. 6 for an antiferromagnet (AFM). As can already be read off from the phase diagram in Fig. 4, there exists a minimum band occupation $n_0(U)$, below which collective magnetism cannot appear. In both cases, FM as well as AFM, n_0 shifts with increasing U to lower values. In the strong-coupling limit ($U \to \infty$) (Ref. 7) we find $n_0(\mathrm{FM}) = 0.44$, $n_0(\mathrm{AFM}) = 0.77$. The magnetization $m(T=0)$ of the FM (Fig. 5) increases very steeply with n, running into the saturation ($m=n$) for $n \geq n_s(U) < 1$, where $n_s(U)$ shifts to lower values for increasing U. This is different in the case of an AFM. It is a typical feature of antiferromagnetic systems that the sublattice magnetization does never reach the saturation. The deviation from saturation for a given n is greater the weaker the Coulomb interaction U. The deviation is reasoned by the fact that the sublattice QDOS of an AFM occupies for both spin directions, $\sigma = \uparrow$ and $\sigma = \downarrow$, exactly the same energy region (see Figs. 14 and 15). Filling the subbands with charge carriers up to the common Fermi edge yields always a finite number of particles with minority spin, resulting in $m < n$. On the other hand, $m \neq 0$ is due to $\rho_{\alpha\uparrow} \neq \rho_{\alpha\downarrow}$. For the FM it may happen under certain conditions that the $\downarrow$ states are all shifted above the Fermi edge, so that $m = n$ holds.

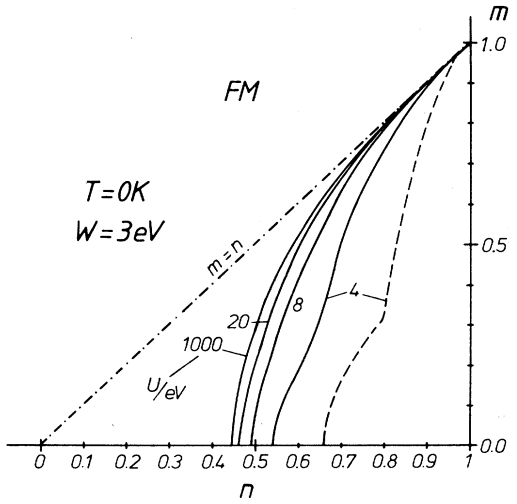

FIG. 5. Magnetization $m = m(T=0)$ of the *ferromagnetic* Hubbard model as function of band occupation n for various values of the Coulomb interaction U ($W=3$ eV). Dashed-dotted line indicates ferromagnetic saturation ($m=n$). The dashed line belongs to the ever existing second solution, which is always less stable than the other one, therefore plotted here as an example only for $U=4$ eV.

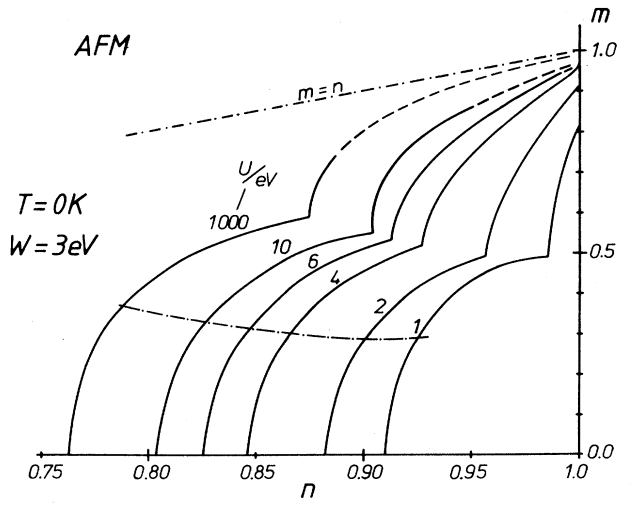

FIG. 6. Sublattice magnetization $m = m(T=0)$ of the *antiferromagnetic* Hubbard model as function of band occupation n for various values of the Coulomb interaction U ($W=3$ eV). Dashed-dotted straight line indicates the never-reached antiferromagnetic saturation ($m=n$). The lower dashed-dotted curve separates first-order (above) and second-order (below) phase transitions.

It should finally be mentioned that for FM a second solution exists, which sets in at a higher n_0 value and never does reach the saturation. It is plotted in Fig. 4 as an example for $U=4$ eV. This solution turns out to be always less stable than the higher-magnetized state. We therefore omit it in the following. A more detailed discussion of this second solution is given in Ref. 7. Its existence seems to be an inherent property of the Hubbard model.[15]

The temperature dependence of the magnetization m of a FM is exhibited in Fig. 7 for several band occupations n and different couplings U/W. We observe first-

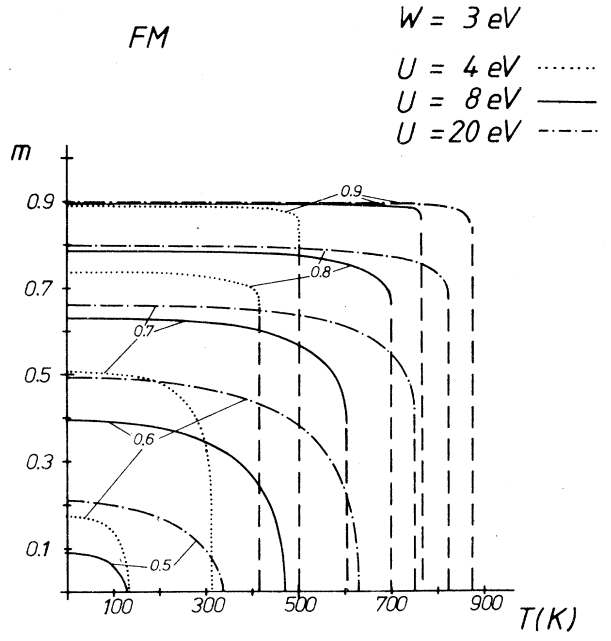

FIG. 7. Magnetization m of the *ferromagnetic* Hubbard model as function of temperature T for three different values of the coulomb interaction U, and various band occupations n, which are plotted as numbers near the respective m-T curve. First-order transitions are indicated by broken lines.

as well as second-order transitions. The closer the carrier concentration to $n=1$, the more likely the transition will be of first order.[7] In all cases $m(T)$ decreases with increasing T.

The temperature behavior of m is especially interesting for an AFM (Fig. 8). We again observe first- as well as second-order transitions, where the latter appear for

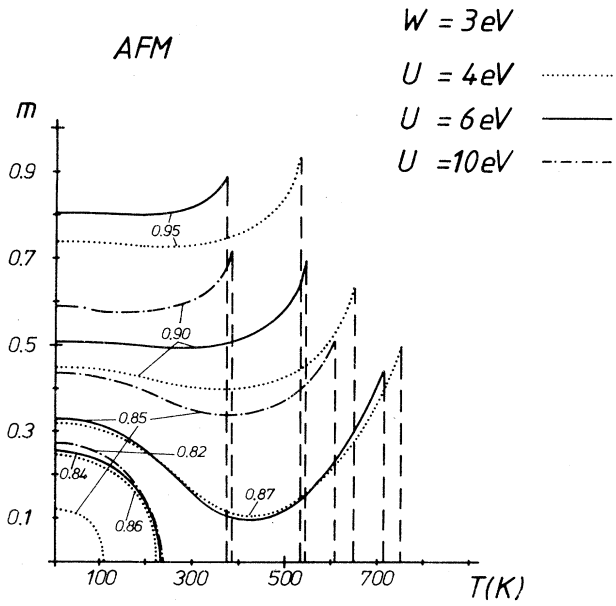

FIG. 8. The same as in Fig. 7, but for the sublattice magnetization of the *antiferromagnetic* Hubbard model.

(U,n) values below the dashed-dotted line in Fig. 6. In the case of a discontinuous transition the magnetization $m(T)$ runs first through a more or less pronounced minimum, after which it increases with increasing T up to the breakdown at T_N. This phenomenon (heat magnetization) is clearly a QDOS -effect. The sublattice QDOS $\rho_{\alpha\sigma}(E)$ is so sensitively dependent on temperature that $\rho_{\alpha\sigma}(E=\mu)$ will strikingly change with T, which may lead to such anomalous $m(T)$ behavior. Similar properties of the Hubbard model have been mentioned in Ref. 20.

C. Critical temperatures

The critical temperatures of a ferromagnetic or antiferromagnetic Hubbard system turn out to be strongly dependent on Coulomb interaction U and band occupation n. Furthermore, the lattice structure plays a non-negligible role.

The Curie temperature T_C of a FM is plotted as a function of U in Fig. 9 and that for various values of n. According to the phase diagram in Fig. 4 there exists for each n a minimum value $U_{\min}(n)$ of the Coulomb interaction at which ferromagnetism sets in. For $U > U_{\min}$, T_C first increases very steeply with U, changing, however, later into a rather flat part. The asymptotic $U \to \infty$ values for the Curie temperatures of the plotted examples

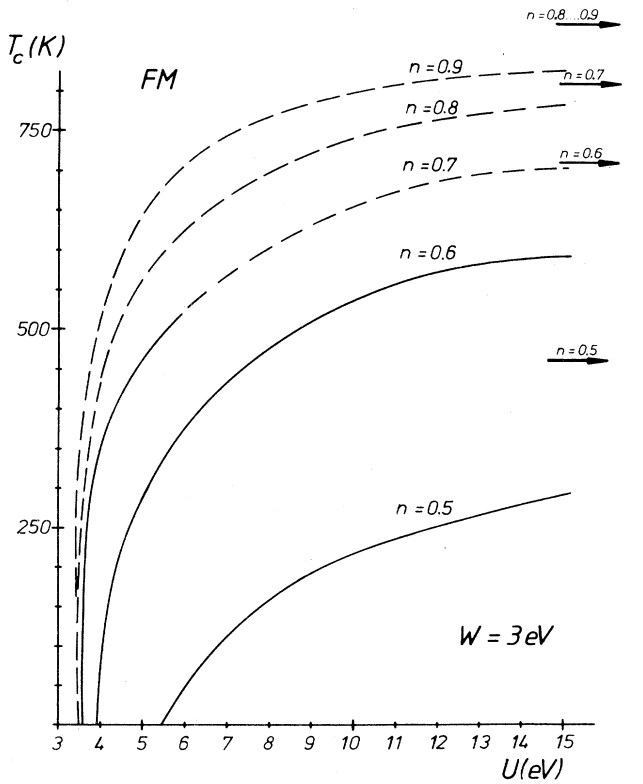

FIG. 9. Curie temperature T_C of the *ferromagnetic* Hubbard model as function of Coulomb interaction U for various band occupations n. Broken lines: first-order transitions; solid lines: second-order transitions. Arrows indicate the $U \to \infty$ values of T_C.

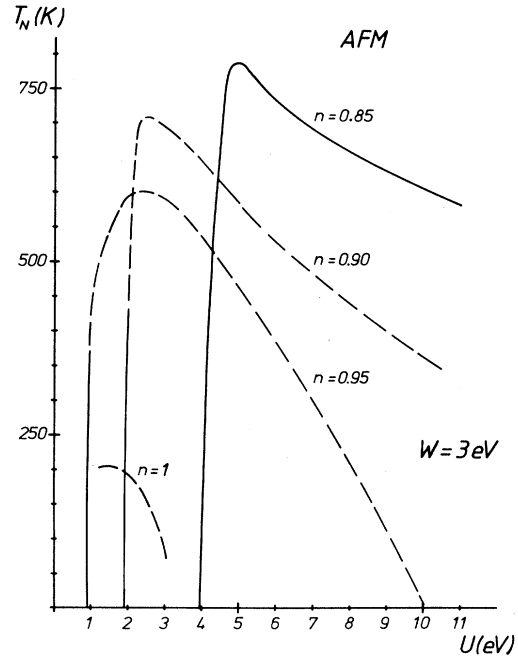

FIG. 10. Néel temperature T_N of the *antiferromagnetic* Hubbard model as function of Coulomb interaction U for various band occupations n. Dashed lines: first-order transitions; solid lines: second-order transitions.

$(0.5 \leq n \leq 0.8)$ lie in between 400 and 800 K. They are, therefore, much more realistic than those of the Stoner model, which typically amount to some 10^4 K (Fig. 2). For a given U, T_C first increases with n (up to $n \simeq 0.9$), runs through a maximum, and decreases again for $n \rightarrow 1$.[7]

Contrary to T_C the Neel temperature T_N of an AFM exhibits a maximum as function of U (see Fig. 10). This points to the fact that antiferromagnetism is obviously favored by intermediate couplings U/W, while ferromagnetism is more stable in the strong-coupling limit $U \rightarrow \infty$. As function of n for fixed U, T_N behaves qualitatively similar to T_C, starting at a minimum band occupation n_0, running through a maximum, and coming down again for $n \rightarrow 1$.

All these results for the critical temperatures T_C and T_N are in remarkable qualitative agreement with those presented in Ref. 33, where a perturbational treatment of the Hubbard model in terms U/W is used for an approximate calculation of the susceptibility χ.

D. Quasiparticle density of states

All the above-presented magnetic properties of the Hubbard model find a natural explanation by the respective behavior of the quasiparticle density of states (QDOS). This function is decisively influenced by four quantities, namely the Bloch density of states (BDOS) $\rho_0(E)$, the Coulomb interaction U, the band occupation n, and the temperature T. For $\rho_0(E)$ we have taken the model function (2.44) plotted as the inset in Fig. 4, while

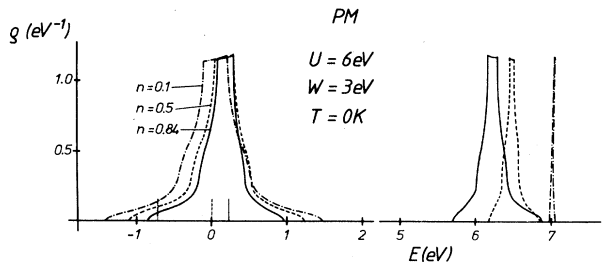

FIG. 11. Quasiparticle density of states of the *paramagnetic* Hubbard model at $T=0$ K as function of energy E for three different values of the band occupation n. Bars mark the corresponding Fermi edges. Parameters are indicated.

U, T, n have been considered as variables.

For all parameter constellations, paramagnetism $(m=0)$ turns out to be a possible mathematical solution of the SDA. In Fig. 11 we have plotted the paramagnetic $T=0$ QDOS for three different band occupations $n=0.1$, 0.5, 0.84, in order to demonstrate its sensitive n dependence. Note, however, that for $n=0.84$ paramagnetism is unstable against ferromagnetism (Fig. 4). The whole spectrum is divided into a low-energy and a high-energy part. Roughly speaking, the low-energy part results from an electron hopping over empty sites, while the high-energy part corresponds to an electron hopping onto sites which are already occupied by an electron of opposite spin. In the latter case the electron must bring up the Coulomb interaction energy. This explains qualitatively why the two subbands are separated by an energy amount of order U (here $U=2W$) and why the width of the lower subband decreases roughly according to $(1-n/2)$ with increasing n while the upper subband becomes broader according to $n/2$. For $n \rightarrow 0$ the upper subband disappears, and the lower subband changes continuously into the free BDOS $\rho_0(E)$.

The mechanism, which creates ferromagnetic order, is strikingly different from that being resposible for an antiferromagnetic order. Figure 12 shows for two different

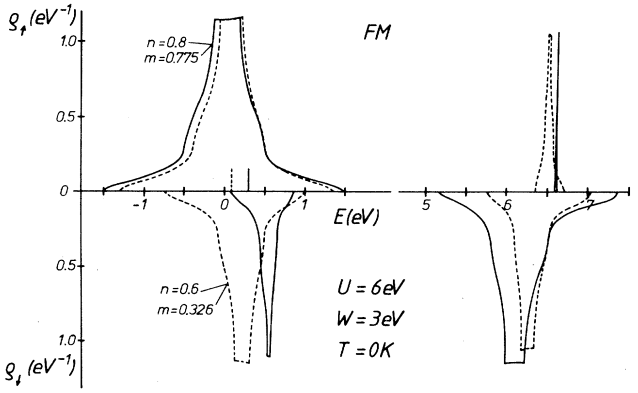

FIG. 12. Quasiparticle densities of states $\rho_\uparrow$ and $\rho_\downarrow$ for the *ferromagnetic* Hubbard model at $T=0$ K as function of the band occupation n. Bars mark the corresponding Fermi edges. Parameters are indicated, in particular the self-consistently calculated magnetization m.

particle concentrations the $T=0$ QDOS of the self-consistent ferromagnetic solution. One observes a remarkable n dependence, mainly due to the very important band shift $B_{S;-\sigma}$, (3.39), which causes a strong spin dependence of the quasiparticle energies $E_{j\sigma p}(\mathbf{k})$ [(3.41)–(3.43)] and of the spectral weights $\alpha_{j\sigma p}(\mathbf{k})$ [(3.44)]. The consequence is that in the low-energy part of the spectrum the ↓ subband is substantially narrowed and also shifted to higher energies compared to the respective ↑ subband. According to (3.46) $\langle n_\uparrow \rangle$ is now greater than $\langle n_\downarrow \rangle$ which means a finite spontaneous magnetization m. The band narrowing of the lower σ subband roughly scales with $(1-\langle n_{-\sigma} \rangle)$. With increasing n the magnetization m grows up (Fig. 5). So the ↑ subband becomes broader with increasing n, reaching the full width W of the Bloch band in the ferromagnetic saturation $m=n$ for $n \geq n_s$. On the other hand, the lower ↓ subband shrinks with increasing n, being finally located completely above the Fermi energy for $n > n_s$, i.e., $\langle n_\downarrow \rangle = 0$. The subbands in the high-energy part of the spectrum which are for $n < 1$ and $U=6$ eV as in Fig. 12, of course unoccupied, behave quite opposite. Their widths scale roughly with $\langle n_{-\sigma} \rangle$. In the ferromagnetic saturation ($\langle n_\uparrow \rangle = n$, $\langle n_\downarrow \rangle = 0$) the upper ↑ subband disappears, because a propagating ↑ electron cannot meet a ↓ electron.

The temperature dependence of the ferromagnetic QDOS comes into play according to our SDA only by Fermi functions. In Fig. 13 we have plotted for a band occupation $n=0.7$ the QDOS for three different temperatures, which demonstrate the transition from ferro- to paramagnetism. It is mainly the lower ↓ subband, which causes the temperature behavior of the magnetization. The ↑ subband does not change so drastically with T. For $T > T_C$, ↑ and ↓ spectrum, of course, coincide, but the upper and lower parts of the spectrum remain separated by a gap of order U. This is the main reason for the realistic T_C values in the SDA (Fig. 9). In the Stoner theory (Fig. 2) the thermal energy has to close a gap of several eV leading to extremely unrealistic Curie temperatures. In the SDA only the relative shift and some kind of deformation of ↑ and ↓ subbands in the lower and higher part, respectively, of the excitation spectrum have to be removed for $T \to T_C$.

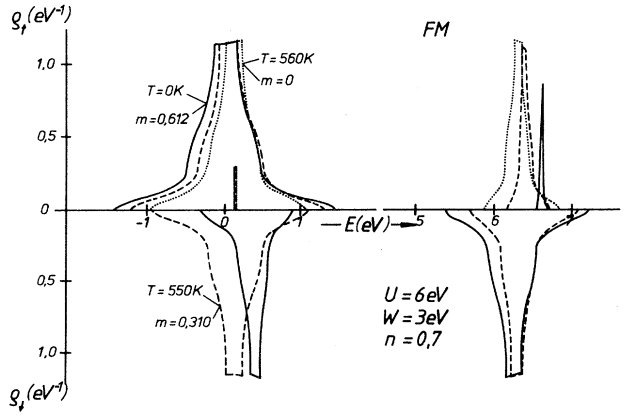

FIG. 13. The same as in Fig. 12, but now for two different temperatures and a fixed band occupation $n=0.7$.

According to our general result (3.50) antiferromagnetic order cannot be caused by a spin dependent shift of the quasiparticle energies as it is the case in the ferromagnetic Hubbard model. In the antiferromagnetic model the quasiparticle energies are spin independent. They are, however, connected with spectral weights, which under certain conditions may be different for ↑ and ↓ electrons. That means that ↑ and ↓ subbands of the sublattice QDOS $\rho_{\alpha\sigma}(E)$ of the antiferromagnetic Hubbard model occupy exactly the same energy regions, but with different state densities. This can be seen in Fig. 14, where we haver plotted $\rho_{A\sigma}(E)$ [$\rho_{B\sigma}(E)$ is identical to $\rho_{A-\sigma}(E)$] for $T=0$ K and for two different band occupations. We observe again, as for paramagnetism (Fig. 11) and for ferromagnetism (Figs. 12 and 13) that the total excitation spectrum is split into a low- and a high-energy part, separated by an energy amount (Hubbard gap) of order U. The sublatticce structure of the antiferromagnet leads, however, to an additional splitting of both parts into subbands, which are classified by the quantum

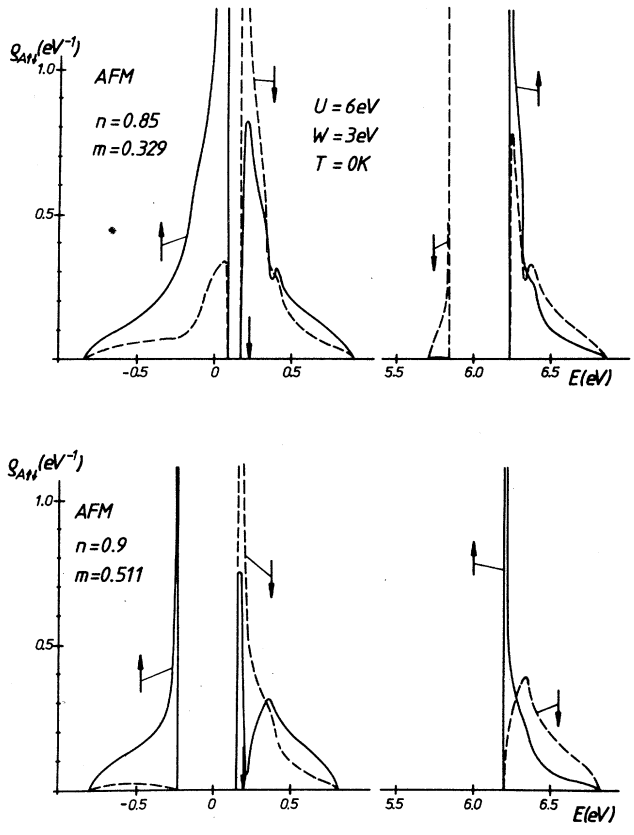

FIG. 14. Sublattice quasiparticle densities of states $\rho_{A\uparrow}$ (solid line) and $\rho_{A\downarrow}$ (broken line) of the *antiferromagnetic* Hubbard model at $T=0$ K as function of energy E. Lower and upper part belong to two different band occupations n. Arrows on the E axis mark the corresponding chemical potentials. Parameters, especially the self-consistently calculated sublattice magnetization m, are indicated.

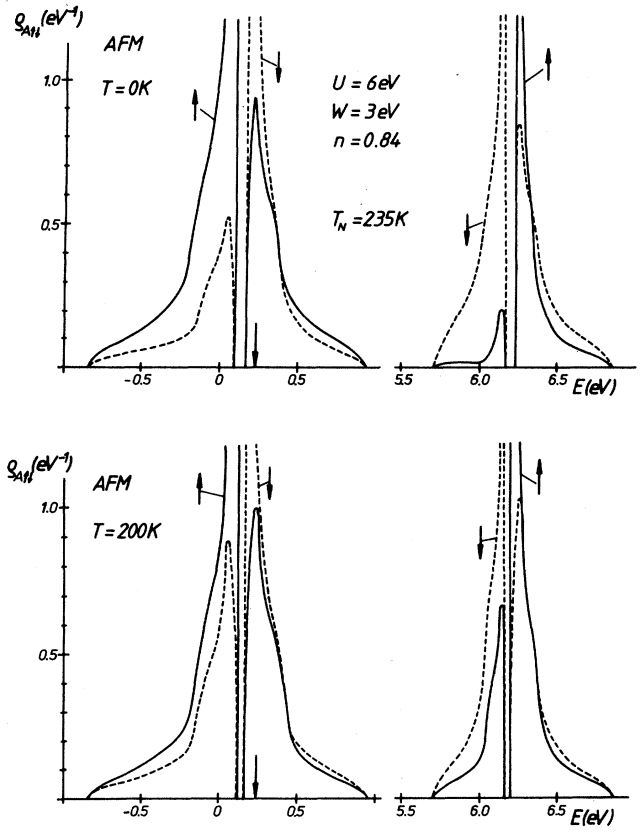

FIG. 15. The same as in Fig. 14, but now for two different temperatures and a fixed band occupation $n=0.84$.

number $p=\mp$ in the quasiparticle energies $E_{j\sigma p}(\mathbf{k})$ [(3.50)]. The gap between the $(j,p=+)$ and $(j,p=-)$ subbands (Slater gap) is greater the higher the sublattice magnetization m and disappears for $m=0$. The $(j,+)$ and $(j,-)$ subbands differ from one another by a change of the majority spin. The actual state density of $\uparrow$ and $\downarrow$ parts are strongly n dependent.

The temperature dependence of a typical sublattice QDOS of the antiferromagnetic Hubbard model is sketched in Fig. 15. The position of the various subbands do not change very much with temperature, only the Slater gap becomes smaller with increasing T, but the QDOS of majority- and minority-spin carriers react extremely sensitive on T. If the chemical potential μ is located within or close to a region of high-state density, then the drastic temperature changes in the QDOS may lead to a nonmonotonic behavior of the sublattice magnetization $m(T)$ (see Fig. 8).

It is again very instructive to compare the QDOS results of the SDA (Fig. 15) with those of the Stoner model (Fig. 3). As in the case of the ferromagnetic Hubbard model (Figs. 2 and 12) the Stoner model suppresses the upper part of the spectrum, while the Slater gap is strongly dependent on the sublattice magnetization, amounting to several eV at $T=0$ K and being closed for $T>T_N$. This leads to an unrealistically high Néel temperature. On the other hand, in the SDA the $m(T)$ behavior results from a pure-state-density effect without a substantial shift of the subbands. T_N is, therefore, smaller by more than one order magnitude in the SDA than in the Stoner model.

Especially interesting is the case $n=1$ for which the chemical potential μ lies in the Hubbard gap at $\mu=U/2$. For the parameters, used in Figs. 14 and 15, the half-filled ($n=1$) Hubbard system is an antiferromagnetic insulator. For $T\rightarrow T_N$ the Slater gap closes, but the Hubbard gap remains rather unaffected. So the system changes from the antiferro- to the paramagnetic phase, but persists to be an insulator. The prototype material for such a behavior is the so-called Mott insulator NiO.[5] In the Stoner model, however, the gap is closed for $T\geq T_N$, so that the system is an insulator below T_N and a metal above T_N. Many one-electron band-structure calculations,[49] based on density-functional theory, use more or less directly a generalized Stoner ansatz for generating the antiferromagnetic structure of NiO. At $T=0$ NiO can be predicted as an insulator, because μ lies in the Slater gap. This picture is, however, completely misleading, since the Slater gap closes for $T\geq T_N$ in the Stoner theory, so that NiO would be a metal in its paramagnetic phase. In our SDA it remains an insulator for all temperatures. We plan to combine the SDA with a self-consistent one-electron band-structure calculation, as we did for the ferromagnetic $4f$ insulator EuO in previous papers[50–52] to get reliable results for the temperature-dependent quasiparticle spectrum of the Mott insulator NiO.

ACKNOWLEDGMENTS

The authors are greatly indebted to Professor Dr. V. Dose for kind hospitality at the Max-Planck-Institut für Plasmaphysik in Garching, Federal Republic of Germany. Financial support of the "Deutsche Forschungsgemeinschaft" is gratefully acknowledged.

*Permanent address: Institute of Physics, Silesian University, Katowice, Poland.

[1]J. Hubbard, Proc. R. Soc. London, Ser. A: **276**, 238 (1963).
[2]J. Hubbard, Proc. R. Soc. London, Ser. A: **277**, 237 (1964).
[3]J. Hubbard, Proc. R. Soc. London, Ser. A: **281**, 401 (1964).
[4]F. Gautier, in *Magnetism of Metals and Alloys,* edited by M. Cyrot (North-Holland, Amsterdam, 1982), p. 1.
[5]B. H. Brandow, Adv. Phys. **26**, 651 (1977).
[6]M. Cyrot, Solid State Commun. **63**, 1015 (1987).
[7]G. Geipel and W. Nolting, Phys. Rev. B **38**, 2608 (1988).
[8]E. Lieb and F. Wu, Phys. Rev. Lett. **20**, 455 (1968).
[9]G. Beni, P. Pincus, and T. Holstein, Phys. Rev. B **8**, 312 (1973).
[10]D. K. Ghosh, Phys. Rev. Lett. **27**, 1584 (1971).
[11]W. Nolting, *Quantentheorie des Magnetismus* (Teubner-Verlag, Stuttgart, 1986), Vol. 2, p. 222.
[12]Y. Nagaoka, Phys. Rev. **147**, 392 (1986).

[13]M. Cyrot, in *Itinerant-Electron Magnetism,* Proceedings of the International Conference, Wadham College, Oxford, 1976, edited by R. D. Löwde and E. P. Wohlfarth (North-Holland, Amsterdam, 1977).
[14]L. M. Roth, Phys. Rev. **184**, 451 (1969).
[15]J. S. Meyer and J. W. Schweitzer, Phys. Rev. B **7**, 4253 (1973).
[16]W. Nolting, Z. Phys. **265**, 173 (1973).
[17]J. Kanamori, Prog. Theor. Phys. **30**, 257 (1963).
[18]P. W. Anderson, Solid State Phys. **14**, 99 (1963).
[19]D. Penn, Phys. Rev. **142**, 350 (1966).
[20]W. Schumacher, U. Lindner, and R. Jauch, Phys. Status Solidi B **86**, 621 (1978).
[21]J. J. Field, J. Phys. C **5**, 664 (1972).
[22]M. Cyrot, J. Phys. (Paris) **33**, 125 (1972).
[23]J. Hubbard, Phys. Rev. B **19**, 2626 (1979).
[24]J. Hubbard, Phys. Rev. B **20**, 4584 (1979).
[25]J. Hubbard, Phys. Rev. B **23**, 5970 (1981).
[26]H. Hasegawa, J. Phys. Soc. Jpn. **46**, 1504 (1979).
[27]H. Hasegawa, J. Phys. Soc. Jpn. **49**, 178 (1980).
[28]T. Moriya and H. Hasegawa, J. Phys. Soc. Jpn. **48**, 1490 (1980).
[29]Y. Kakehashi and P. Fulde, Phys. Rev. B **32**, 1595 (1985).
[30]M. C. Gutzwiller, Phys. Rev. **137**, A1726 (1965).
[31]Y. Kakehashi and H. Hasegawa, Phys. Rev. B **36**, 4066 (1987).
[32]K. Kubo, Prog. Theor. Phys. **64**, 758 (1980).
[33]B. H. Zhao, H. Q. Nie, K. Y. Zhang, K. A. Chao, and R. Micnas, Phys. Rev. B **36**, 2321 (1987).
[34]H. Shiba and P. Pincus, Phys. Rev. B **5**, 1966 (1972).
[35]Z. G. Soos and S. Ramasesha, Phys. Rev. B **29**, 5410 (1984).
[36]J. E. Hirsch, Phys. Rev. B **31**, 4403 (1985).
[37]J. E. Hirsch, Phys. Rev. B **35**, 1851 (1987).
[38]J. Callaway, D. P. Chen, and Y. Zhang, Phys. Rev. B **36**, 2804 (1987).
[39]W. Nolting and A. M. Oleś, J. Phys. C **13**, 2295 (1980).
[40]W. Nolting and A. M. Oleś, Phys. Rev. B **22**, 6184 (1980).
[41]W. Nolting and A. M. Oleś, Physica **143A**, 296 (1987).
[42]See, e.g., Ref. 11, p. 289.
[43]O. K. Kalashnikow and E. S. Fradkin, Phys. Status Solidi B **59**, 9 (1973).
[44]L. S. Campagna, M. D'Ambrosio, and U. Espositio, J. Phys. **18**, 6219 (1985).
[45]A. B. Harris and R. V. Lange, Phys. Rev. **157**, 295 (1967).
[46]T. Ogawa, K. Kanda, and T. Matsubara, Prog. Theor. Phys. **53**, 614 (1975).
[47]T. Takano and M. Uchinami, Prog. Theor. Phys. **53**, 1267 (1975).
[48]J. Florencio and K. A. Chao, Phys. Rev. B **14**, 3121 (1976).
[49]K. Terakura, T. Oguchi, A. R. Williams, and J. Kübler, Phys. Rev. B **30**, 4734 (1984).
[50]W. Nolting, G. Borstel, and W. Borgieł, Phys. Rev. B **35**, 7015 (1987).
[51]W. Nolting, W. Borgieł, and G. Borstel, Phys. Rev. B **35**, 7025 (1987).
[52]W. Nolting, W. Borgieł, and G. Borstel, Phys. Rev. B **37**, 7663 (1988).